



Comparative Study between *Croton tiglium* Seeds and *Moringa oleifera* Leaves Extracts, after Incorporating Silver Nanoparticles, on Murine Brains



CrossMark

Wael M. Aboulthana^{a,*}, Ahmed M. Youssef^b, Mohamed M. Seif^{c,d}, Noha M. Osman^e, Ram K. Sahu^f,
Mohamed Ismael^g, Hatim A. El-Baz^a, Nagwa I. Omar^a

^a Biochemistry Department, Genetic Engineering and Biotechnology Research Division, National Research Centre, 33 El Bohouth St. (former El Tahrir St.), Dokki, Giza, P.O. 12622, Egypt.

^b Packaging Materials Department, National Research Centre, 33 El Bohouth St. (former El Tahrir St.), Dokki, Giza, P.O. 12622, Egypt.

^c Toxicology and Food Contaminants Department, Food Industries and Nutrition Research Division, National Research Centre, 33 El Bohouth St. (former El Tahrir St.), Dokki, Giza, P.O. 12622, Egypt.

^d College of Animal Science and Technology, Northwest A&F University, Yangling, Shaanxi, 712100, China.

^e Cell Biology Department, Genetic Engineering and Biotechnology Research Division, National Research Centre, 33 El Bohouth St. (former El Tahrir St.), Dokki, Giza, P.O. 12622, Egypt.

^f Department of Pharmaceutical Science, Assam University (A Central University), Silchar-788011, Assam, India.

^g Energy and Environmental Sciences Laboratory, Chemistry Department, Faculty of Science, Sohag University, Egypt.

Abstract

Croton tiglium seeds and *Moringa oleifera* leaves extracts are rich in phytoconstituents with the antioxidant efficiency which can be enhanced by incorporating silver nanoparticles (Ag-NPs). The present study was designed to compare the effect of *C. tiglium* seeds and *M. oleifera* leaves nano-extracts on brain tissues of murine models. During the current study, acetylcholine esterase (ACHE), β -amyloid (A β) content and inflammatory markers were measured in brain tissues. Moreover, native protein, lipoprotein and isoenzymes patterns were electrophoretically detected. Also, the interferon-gamma (INF- γ) receptor protein was studied by molecular dynamic simulation to evaluate the significant alterations on brain tissues. It was found that ACHE, A β contents and inflammatory markers increased in *C. tiglium* nano-extract treated group at a dose of 6.5 ml/kg. Furthermore, it caused qualitative electrophoretic abnormalities represented by lowering similarity index (SI) values. Also, the residues range 119~127 represent the most reactive and flexible site in INF- γ receptor protein. On the other hand, it was shown that no significant differences were induced by silver *M. oleifera* nano-extract.

Keywords: *Croton tiglium* Seeds; *Moringa oleifera* Leaves; Nanotechnology; Electrophoresis; Molecular Dynamic Modelling.

1. Introduction

Croton tiglium plays an effective role in ethnomedicine for treatment of several cancer diseases [1]. It belongs to the family Euphorbiaceae that includes about 280 genera and 8000 species [2]. Moreover, *C. tiglium* seeds extracts are rich in various active phytochemicals such as ascorbic acid, tocopherol and other pigments. All these phytoconstituents are responsible for the antioxidant efficiency of the plant extract [3].

It is well known that *C. tiglium* seeds are characterized by the presence of phorbol esters,

crotonic acid, fatty acids and active phytoconstituents, which are responsible for severe purgative effect of the *C. tiglium* seeds extract [4]. In addition to, croton oil which is rich in 12-O-tetradecanoylphorbol-13-acetate and exhibits the most effective role in inhibiting growth and stimulating apoptosis in solid tumors [5]. On the other hand, a study by El-Kamali *et al.* [6], reported that aqueous *C. tiglium* seeds extracts have no significant alterations in the biochemical

*Corresponding author e-mail: wmkamel83@hotmail.com.; (Wael M. Aboulthana).

Receive Date: 15 December 2020, Revise Date: 31 December 2020, Accept Date: 03 January 2021

DOI: 10.21608/EJCHEM.2021.53777.3113

©2021 National Information and Documentation Center (NIDOC)

measurements, but they have little effect on some haematological indices.

Moringa oleifera belongs to the family *Moringaceae* that includes about 13 known species under the same genus [7]. *M. oleifera* leaves and seeds extracts exhibited antioxidant efficiency against deleterious effects induced by oxidative stress and free radicals attack [8]. Moreover, they are rich in variety of essential phytochemicals such as total phenolics, vitamins and various enzymes as catalase, polyphenol oxidase and ascorbic acid oxidase [9]. Moreover, they contain flavonoids, tannins, saponins, sterols, anthraquinones, alkaloids, terpenoids and reducing sugars that exist along with anti-cancerous agents like isothiocyanates, glucosinolates, glycoside compounds and glycerol-1-9-octadecanoate [10]. Kirisattayakul *et al.* [11] demonstrated that *M. oleifera* leaves extract ameliorated brain dysfunctions induced by oxidative stress. Recently, Leone *et al.* [12] evaluated the active phyto-constituents isolated from *M. oleifera* leaves against cancer activity with respect to tumor-suppressive activity.

Nanotechnology is a relatively new branch of science that has found a wide range of applications in medical research. Nanoparticles are the keystones of nanotechnology and have physical characteristics such as shape and size. These unique properties enable it to be applied in fundamental research fields [13]. The incorporation of metal nanoparticles into plant extracts showed valuable properties in many practical applications especially these incorporated plant extracts exhibited high antioxidant efficiency at lower concentrations [14].

The elevation of the antioxidant activity of plant nano-extracts referred to increasing the total polyphenolic compounds and other active phyto-constituents after incorporating silver nanoparticles (Ag-NPs) [15]. Moreover, there is no obvious toxicity occurred in animal organs after oral administration of the silver plant nano-extracts [16]. This might be related to the efficiency of the kidneys to remove nanoparticles from the body by mean of renal clearance. Therefore, the chance for nanoparticles to undergo catabolic process decreased and hence the possible side effects were avoided [17]. On the other hand, De Jong *et al.* [18] postulated that brain is considered as one of the most organs susceptible to deposition of the nanoparticles.

Interferon-gamma (INF- γ) receptor protein plays an effective role in protecting the brain through its activation in concert with the other proinflammatory cytokines [19]. It is a critical component of immunological defense against the adverse effect on the central nervous system [20]. It provides a novel tool to reveal impact of the intracellular signalling induced by INF- γ on the elimination of deleterious

effect and microbial pathogens targeting glial cells, and mechanisms of demyelination and remyelination [21]. It is composed of two subunits expressed by somatic cells to induce a diversity of effects and intracellular signaling depending on the target cells [22]. The present study aims to compare the effect between *C. tiglium* seeds and *M. oleifera* leaves extracts incorporated by Ag-NPs to evaluate the significant alterations on brain tissues of murine models.

2. Materials and Methods

2.1. Preparation of aqueous plant extract

C. tiglium seeds and *M. oleifera* leaves were dried and powdered then extracted by distilled water. The extracts were separately filtered then concentrated at 50°C under reduced pressure using a rotary evaporator.

2.2. Preparation of silver *C. tiglium* seeds and *M. oleifera* leaves nano-extracts

The Ag-NPs were prepared by reducing silver nitrate (AgNO₃) with ethylene glycol (EG) in existence of polyol as suggested by Aboulthana *et al.* [23]. During the experiment, EG (10 ml) was refluxed at 160 °C for 25 min. Consequently, 5 ml of AgNO₃ solution in EG and 10 ml of 0.15 M PVP solution in EG containing 0.03 mM MnCl₂ were concurrently injected into flask for 10 min. The reaction mixture was refluxed and vigorously stirred at 160 °C for 60 min then followed by cooling the reaction mixture to room temperature. The reaction product was centrifuged at 3000 rpm for 5 min then washed with acetone and ethanol for three times. The Ag-NPs were collected and dried at 70 °C then the Ag-NPs were added to *C. tiglium* seeds and *M. oleifera* leaves extracts at different concentrations to form silver plant nano-extracts.

2.3. Characterization of the prepared Ag-NPs

2.3.1. X-Ray Diffraction (XRD)

The crystal structure of the synthesized Ag-NPs was determined by a Philips X-ray diffractometer (PW 1930 generator, PW 1820 goniometer) that equipped with Cu K α radiation (45 kV, 40 mA, with $\lambda = 0.15418$ nm). The analysis scans were run in 2 θ range of 5 to 80° with 0.02 step size and 1s step time.

2.3.2. Transmission Electron Microscope (TEM)

The synthesized Ag-NPs were characterized morphologically in addition to determining the particles size using TEM (JEM-1230, Japan) operated at 120 kV with resolution until 0.2 nm and maximum magnification of 600X10³. Before characterization, aqueous sample dispersion (one drop) was placed on

a carbon-coated copper grid then allowed in air to dry.

2.3.3. Ultraviolet-visible (UV-VIS) spectroscopy

The silver nitrate (AgNO_3) that reduced by plant extracts was monitored by measuring UV-VIS spectrum of the reaction mixture at λ 200–800 nm after 10-fold dilution of the samples with deionized water. The UV-VIS spectroscopy was carried by Shimadzu UV-Vis recording spectrophotometer UV-240.

2.3.4. Dynamic Light Scattering (DLS)

Distribution of the synthesized Ag-NPs was investigated by photon correlation spectroscopy (PCS) using Malvern Zetasizer Nano ZS (Malvern Instruments Ltd., Malvern, UK) after diluting the samples with deionized water prior to analysis at room temperature with an angle of detection of 90° .

2.4. Experimental Design

2.4.1. Ethical approval statement

The experimental design and animals handling were carried out according to guidelines reported in "Guide for the care and use of laboratory animal" and based on protocol approved by Institutional Animal Ethical Committee of National Research Centre, Dokki, Giza, Egypt (No: 475/2019).

2.4.2. Administration of nano-extracts

The plant extracts and their silver nano-extracts were administrated orally by stomach tube based on the median lethal doses (LD_{50}) which were determined in the *C. tiglium* seeds extract and its nano-extract which were about 85 and 65 ml/kg b.w., respectively [23]. For *M. oleifera* leaves, the LD_{50} values of the extract and its nano-extract were about 14.25 and 13.75 mg/Kg b.w., respectively [24].

2.4.3. Animals and treatments

Healthy forty-nine (49) adult male *Sprague Dawley* rats weighting between 120-150 g were randomly divided into 7 groups (7 rats per cage). They were housed and maintained under normal nutritional and environmental conditions in Animal House of National Research Center, Cairo, Egypt.

Control group: rats were fed with normal diet and received tap water for 12 weeks. *C. tiglium* seeds extract treated group: rats were fed with normal diet associated with administration of *C. tiglium* seeds extract orally at dose equivalent to 1/10 of LD_{50} (8.5 ml/kg b.w.) by stomach tube for 12 weeks. Silver *C. tiglium* seeds nano-extract treated group: this group can be subdivided according to dose of nano-extract into two subgroups. Rats were fed with normal diet associated with administration of *C. tiglium* seeds

nano-extract orally at dose of 3.3 ml/kg b.w. (1/20 of LD_{50}) for 12 weeks. Rats were fed with normal diet associated with oral administration of *C. tiglium* seeds nano-extract at a dose of 6.5 ml/kg b.w. (1/10 of LD_{50}) for 12 weeks. *M. oleifera* leaves extract treated group: rats were fed with normal diet associated with oral treatment with aqueous *M. oleifera* leaves extract at a dose of 1.4 g/kg b.w. (1/10 of LD_{50}) for 12 weeks. Silver *M. oleifera* leaves nano-extract treated group: this group can be subdivided according to dose of the nano-extract into two subgroups. Rats were fed with normal diet associated with administration of *M. oleifera* leaves nano-extract orally at a dose of 0.7 g/kg b.w. (1/20 of LD_{50}) for 12 weeks. Rats were fed with normal diet associated with oral administration of *M. oleifera* leaves nano-extract at a dose of 1.4 g/kg b.w. (1/10 of LD_{50}) for 12 weeks.

2.5. Samples collection

At end of the experiment, rats were fasted for 18 hrs and anesthetized by slight exposure to diethyl ether to be sacrificed by cervical dislocation. Brain tissues were excised and split into two portions. Portion I washed immediately in ice-cold saline and rapidly frozen in liquid nitrogen then homogenized in Tris-HCl buffer (0.01 M and pH 7.4). The clear supernatants were transferred to new tubes after centrifuging the homogenates at 10,000 rpm for 15 min and split into separated aliquots then kept at -20°C in clean stoppered vials until biochemical and electrophoretic assays. Portion II was frozen at -80°C for DNA extraction.

2.5.1. Biochemical assays

Brain acetylcholine esterase (ACHE) activity and brain β -amyloid ($\text{A}\beta$) content were assessed in brain tissues homogenates using ELISA Kits (USCN Life Science, Inc. (Product Number MBS702915)). In addition, markers of oxidative stress were quantified in clear supernatants of brain tissue homogenates. These assays including: i) Products of the peroxidation reactions: Protein carbonyl content (PCC) (protein oxidation product) was assayed spectrophotometrically in brain tissue and expressed as nmol of reactive carbonyl compounds per mg protein of tissue [25]. Lipid peroxidation product (LPO) was determined as malondialdehyde (MDA) that is the end product of peroxidation reaction and the result was expressed as (nmol/g wet tissue) [26]. Nitrite level (an Index of Nitric Oxide) was measured by colorimetric method using Griess reagent [27]. ii) Antioxidants: Total Antioxidant Capacity (TAC) was determined and expressed as mM/L [28].

Activities of superoxide dismutase (SOD) [29], catalase (CAT) [30], glutathione peroxidase (Gpx) activity [31] and level of reduced glutathione (GSH)

[32] were spectrophotometrically quantified. Moreover, markers of inflammatory reactions including interleukin-1 β (IL-1 β) [33] and tumor necrosis factor- α (TNF- α) [34] were assessed using quantitative sandwich enzyme immunoassay technique.

2.6. Statistical analysis

The statistical analysis was carried out by one-way analysis of variance test (one-way ANOVA) followed by Bonferoni test using Statistical Package for Social Sciences (SPSS for windows, version 11.0). The results were expressed in tables and figures as mean \pm standard error (SE). The differences were considered statistically significant when a "P" value was less than 0.05.

2.7. Electrophoretic Patterns

Equal volumes of the individual supernatants in each group were mixed together in one tube and used as one sample. Concentration of total protein was assayed in all samples [35]. During the electrophoretic assays, the samples loaded in all wells with equal protein concentrations.

2.7.1. Native protein patterns

Native proteins were electrophoretically separated using Polyacrylamide Gel Electrophoresis (PAGE) based on the methods documented by Laemmli [36] and modified by Darwesh *et al.* [37] who reported that samples, gels and running buffers contained no sodium dodecyl sulphate. The native protein bands were stained by Commassie Brilliant Blue G-250 and visualized as blue bands. The lipid moieties of native protein were stained by Sudan Black B (SBB) visualized as black bands [38].

2.7.2. Isoenzymes

The isoenzymes were electrophoretically detected through identification of the enzyme subunits. Firstly, electrophoretic catalase pattern (CAT) and electrophoretic peroxidase (POX) pattern were assayed for native gel after electrophoretic run by incubating with H₂O₂ as substrate then stained. The stained CAT subunits appeared as yellow bands in the gel [39]. While, the stained POX subunits appeared as brown bands in the gel [40]. Finally, esterase (EST) pattern was electrophoretically detected according to the method suggested by Ahmad *et al.* [41] to localize in-gel EST activity by incubating gel in conditioning buffer followed by reaction mixture containing α , β -naphthyl acetate (5.58×10^{-3} mM, pH 7.5) along with Fast Blue RR (dye coupler). The α -naphthyl acetate used as substrate for α -esterases which appeared as brown

bands and β -naphthyl acetate used as substrate for β -esterases which appeared as dark pink bands.

2.7.3. Genomic DNA pattern

The genomic DNA was extracted from brain tissues according to the method documented by Barker *et al.* [42]. Concentration and purity of the DNA yield were estimated by NanoDrop® spectrophotometer (ND-1000, NanoDrop Technologies Inc, Delaware, USA). The DNA purity was considered to be accepted when its value is ranged between 1.8 - 2.0. The value of less than 1.8 indicates that DNA yield contaminated with protein and a ratio of >2.0 indicates contamination with RNA. Integrity of the genomic DNA was assayed using gel electrophoresis (Bio-Rad, USA) by resolving DNA extracts on a 1.5% agarose containing ethidium bromide. The DNA bands were visualized on a UV transilluminator and analyzed in comparison to DNA molecular weight marker (HyperLadder II) with regularly spaced bands ranging from 50 bp to 2000 bp.

2.7.4 Data analysis

The PAGE and agarose gel plates were scanned then analyzed by the Quantity One software (Version 4.6.2) that was used to determine the relative mobility (Rf), band percent (B%) and band quantity (quant.) of the bands separated electrophoretically. In addition, the similarity index (SI%) and genetic distance (GD%) were calculated to compare all treated groups to control group.

2.7.5. Molecular Dynamic Modelling

Protein sequence of interferon- γ (INF- γ) receptor was retrieved from National Center for Biotechnology Information (NCBI) database at <https://www.ncbi.nlm.nih.gov/protein>, in FASTA format. The sequence had been selected taking in consideration the rat organism and brain tissue to represent the empirical data used in the experimental work. Secondary structure was derived using POLYVIEW which estimated the rigid helical, sheet and flexible coil regions of the protein sequence [43]. Threading templates had been selected using restraint-based comparative with templates in FASTA and BLAST databases [44,45]. Using this preliminary analysis, 3D model was build using automated I-TASSER software server [46,47]. Basically, it utilized multiple-threading alignment with interactive assembly simulation with an accuracy predicting function (C-score) based on alignment quality and energy convergence. The best constructed model of I-TASSER was further refined using Galaxy Refine software [48], in this simulation all side chains were reconstructed and repacked with

structural relaxation using mild molecular dynamics simulation.

3. Results and Discussion

It is well known that the Ag-NPs gained boundless interests among all noble metal nanoparticles due to their characteristic properties in addition to their significant antibacterial, antiviral, antifungal and anti-inflammatory effects. Moreover, silver a nontoxic, safe inorganic antibacterial agent that is capable of killing about 650 types of diseases causing microorganisms and it exhibits an effective biocidal effect as antiseptic against various microorganisms through disruption of the unicellular membrane and the enzymatic activities [49]. The recent studies documented that incorporation of Ag-NPs into the plant extract showed higher antioxidant properties due to increase the active phytoconstituents with significant free radical scavenging activity [50]. In addition, Abdelhady and Badr [51] reported that antioxidant capacity is correlated with anticancer activity. The recent studies reported that synthesis of Ag-NPs using plant extracts is energy efficient and cost effective [52]. In the current study, *C. tiglium* seeds and *M. oleifera* leaves extracts were incorporated with Ag-NPs to measure the antioxidant efficiency of these extracts after incorporation which would be help in therapeutic purposes.

The XRD and TEM are considered as the most significant techniques suitable to examine structural properties of the fabricated nanomaterials. In the current study, The Ag-NPs were prepared and studied using the XRD diffraction pattern. Data illustrated in Fig. 1a showed that XRD result of the prepared Ag-NPs displayed the characteristic peaks of metallic Ag⁰ found at 37.8°, 44.5° and 67.6° matching with the crystallographic planes (1 1 1), (0 0 2) and (0 2 2) of Ag-NPs, respectively and generates a typical of crystalline metallic Ag phase. Moreover, the XRD displayed separate diffraction peaks around 37.8°, which are indexed by the (002) of the cubic face-centered silver. These sharp Bragg peaks may be displayed as a result of capping agent used for stabilizing the prepared Ag-NPs. Strong Bragg reflections recommended that strong X-ray scattering centers in the crystalline phase and might refer to capping agents. An increase in the incubation time with Ag-NO₃ solution along with plant extract increased during synthesis of Ag-NPs. Presence of the plant extract reduced formation of AgNO₃ into Ag ions. Also, the secondary metabolites present in the plant extract act as a reducing agent during Ag-NPs synthesis [53]. In addition to, TEM technique was used to evaluate the shape, size and morphology of nanoparticles. As revealed in Figs. 2b & 2c, it was noticed that Ag-NPs were predominantly spherical in their shapes. Although Ag-NPs were well dispersed, some of the NPs were irregular in shape. No

aggregations were detected. Furthermore, based on the morphological data obtained using TEM, it was demonstrated that the Ag-NPs were formed as a result of the chemical reduction which was carried out in presence of AgNO₃ solution. Presence of Ag-NPs maintained the homogeneity and uniformity of Ag-NPs distribution in particles size range (5-10 nm) as illustrated in the TEM image. This was in agreement with findings of the study carried out by Aboulthana *et al.* [23].

The Ag-NPs have exceptional optical properties that generate strongly interrelate with exact wavelengths of light. As illustrated in Fig. 2d, the synthesized Ag-NPs showed a sharp peak at 450 nm that confirms formation of the Ag-NPs. Consequently, DLS is a nondestructive technique used to acquire the average diameter of the prepared dispersed nanoparticles in aqueous solutions. It is mostly used to determine particles sizes and their distribution in aqueous solutions. Moreover, as shown in Fig. 2e, the particles sizes distribution of synthesized Ag-NPs have main diameter around 82 nm. In addition to, particles sizes obtained from DLS were larger than the ones obtained from TEM. This might be attributed to the effect of Brownian motion and Ag-NPs agglomeration. Furthermore, these synthesized Ag-NPs exhibited good stability due to presence of secondary metabolites as a capping or reducing agent [54].

It was reported that Ag-NPs exhibit their adverse effect on the brain directly *via* trans-synaptic transport or through disruption of the blood-brain barrier and then accumulate in brain regions [55]. As illustrated in Fig. 2, the incorporation of Ag-NPs into *M. oleifera* leaves extract caused no significant differences in biochemical measurements such as ACHE and Aβ contents of brain tissues when compared to control and *M. oleifera* leaves extract treated groups. On the other hand, incorporation of Ag-NPs into *C. tiglium* seeds extract caused significant elevation of these measurements levels in brain tissues when it was administrated at a dose of 6.5 ml/kg as compared to control and *C. tiglium* seeds extract treated groups. This significant elevation due to binding of Aβ to nicotinic receptors directly which leads to increase ACHE contents in and around Aβ deposits as reported by Ahmed *et al.* [56]. Moreover, elevation of the Aβ level results in increased the ACHE content in and around Aβ plaques. The Aβ deposits were co-localized by ACHE and this consequently leads to promoting assembly of the Aβ into amyloid fibrils producing Aβ-ACHE complex that is more toxic than amyloid fibrils [57]. Consequently, elevation of the PCC and the neurotoxicity occur as a result of elevation of the Aβ that involves in formation of the reactive oxygen species (ROS). In addition, aggregation of Aβ by

mean of self-aggregation leads to generation of the hydroxyl radicals ($\cdot\text{OH}$) that consequently induce the peroxidation reactions leading to disrupting the neuronal membranes and oxidation of the macromolecules like lipids, proteins and nucleic acids [58].

Lipid peroxidation is considered as one of the most common reasons of oxidative damage that induced brain tissue toxicity. Thiobarbituric acid reactive substances (lipid peroxidation product) and PCC are the most common markers of oxidative stress which indicate to the effect of ROS on lipids and proteins [59]. Brain is rich in unsaturated fatty acids that susceptible to free radicals' attacks [60]. The oxygenate radicals are able to interrupt the cellular integrity and performance [61]. It was established that the nanoparticles bind tightly to ATP synthase in brain and this consequently leads to mitochondrial dysfunction and hence impairment of the ATP production. The mitochondrial dysfunction is strongly related to ROS production [62]. Thereafter, the oxidative stress occurred as a result of the exposure to Ag-NPs leads to tissue toxicity and this might be attributed to mitochondrial dysfunction induced by its interaction with proteins during ATP production [63]. The GSH is a non-enzymatic antioxidant exhibiting an effective scavenging role against attack of the free radicals *via* its $-\text{SH}$ group [64]. The antioxidant enzymes play an important role in the brain tissues to avoid the deleterious effects induced by attack of these radicals [65]. As shown in **Table 1**, incorporation of Ag-NPs into *M. oleifera* leaves extract caused no significant variations in non-enzymatic biomarkers of the oxidative stress such as LPO, TAC, GSH and nitrite in brain tissues with respect to control and *M. oleifera* leaves extract treated group. While, incorporation of Ag-NPs into *C. tiglium* seeds extract showed neurotoxic effect in brain tissues when administrated at a dose of 6.5 ml/kg due to elevation levels of LPO and nitrite biomarkers significantly ($P < 0.05$).

Levels of LPO and nitrite increased significantly ($P < 0.05$) associated with decline in TAC and GSH levels in brain tissues of rats treated with silver *C. tiglium* seeds nano-extract at the dose 6.5 ml/kg. The oxidative stress occurred in that tissues due to imbalance in the antioxidant system between ROS generation and antioxidant capacity and hence leads to neurodegenerative disorders [66]. Enhancement of the ROS generation is usually related to stimulating LPO through converting polyunsaturated fatty acids into toxic lipid peroxides in the cell membrane. This consequently leads to destruction of the membrane and hence cell injury [67].

Nitric oxide (NO) exhibited cytotoxic effect by interaction of the macromolecules such as lipids and

DNA with oxygen forming nitrosative species such as peroxy nitrite by oxidation, nitrosation or nitration [68]. In current study, there was an elevation in nitrite level in silver *C. tiglium* seeds nano-extract treated group with a dose of 6.5 ml/kg.

As a result of the treatment with silver *C. tiglium* seeds nano-extract at a dose of 6.5 ml/kg, elevation of nitrite might reflect the increased production of NO with nitrosative influence on the brain. Antioxidant enzymes work together to antagonist oxidative stress. During this mechanism, SOD catalyzes dismutation of the superoxide radical into hydrogen peroxide that decomposed consequently to non-toxic products (water and oxygen) by CAT [69].

Data in **Table 2** showed that no significant differences noticed in activities of antioxidant enzymes such as SOD, CAT and Gpx in brain tissues of rats treated with silver *M. oleifera* leaves nano-extract at both doses (0.7 and 1.4 g/kg). On the other hand, silver *C. tiglium* seeds nano-extract treated group with a dose of 6.5 ml/kg showed significant decrease in activities of antioxidant enzymes ($P < 0.05$) in brain tissues when compared to control, *C. tiglium* seeds extract treated group and silver *C. tiglium* seeds nano-extract treated group with a dose of 3.3 ml/kg. This was in agreement with Afifi *et al.* [70] who suggested that expression of antioxidant enzymes genes deteriorated in brain tissues as a result of the exposure to high Ag-NPs concentrations. Moreover, depletion of the GSH, SOD and CAT in silver *C. tiglium* seeds nano-extract treated rats (6.5 ml/kg) might be related to their consumption during ROS elimination and inhibiting nitrosative stress [67].

As revealed in **Table 3**, it was found that incorporation of Ag-NPs into *M. oleifera* leaves extract caused no significant differences in levels of the inflammatory markers (IL- 1β and TNF- α) in brain tissues of rats treated with the nano-extract at both doses (0.7 and 1.4 g/kg) with respect to control and *M. oleifera* leaves extract treated group. On the other hand, it was emphasized that silver *C. tiglium* seeds nano-extract caused no significant difference in the inflammatory markers when administrated at a dose of 3.3 ml/kg. Furthermore, levels of these markers elevated significantly ($P < 0.05$) in brain tissues of rats treated with the nano-extract at the dose 6.5 ml/kg. In consistent with our results in which the enzymatic and non-enzymatic antioxidants decreased in association with elevation of LPO and nitrite levels following the treatment with silver *C. tiglium* seeds nano-extract (6.5 ml/kg) increased concentrations of the inflammatory markers (IL- 1β and TNF- α) in that tissues. These findings were supported by results obtained by Ansar *et al.* [63] who found that the nanoparticles lead to "neurotoxicity" following oral

exposure via oxidative and inflammatory mechanisms. During the oxidative and nitrosative stress, the inflammatory mediators expression was upregulated and triggered through activation of transcription factor (nuclear factor kappa-B) [71]. Furthermore, Shim *et al.* [72] reported that the activated inflammatory proteins detected on surface of the nanoparticles that may play a role in inflammatory reaction in brain tissues after its oral administration.

It was found that electrophoresis acts as a tool to identify the specific proteins which expressed in the different tissues. The differences detected electrophoretically may occur qualitatively through disappearance in some protein bands or appearance of new ones. Disappearance of the normal protein bands might be attributed to the adverse effect of the toxic substance which inhibits expression of the genes responsible for synthesis of these deleted proteins. Moreover, the band remained with normal identification data (Rf) but it usually differs in the band amount (B% and Quant.). This may be explained by the toxic substance could not inhibit synthesis of this protein type but it may be affected only at the quantitative level [73, 74]. Therefore, values of the similarity index and genetic distance between the control and the other treated groups related to number and arrangement of the bands. The SI is only correlated to the physiological state of tissue and it is inversely proportional to the genetic distance [75].

Proteins are the most important macromolecules in all living cells. They may be essential for cell division (as nucleoproteins) and for control many reactions in the metabolic pathways (as enzymes and hormones). Thus, separation and characterization of the individual proteins are necessary to facilitate study of the chemical nature and physiological function of each protein. In the brain tissues, the proteins were separated electrophoretically and abundances were measured by using image analysis technique [73].

As presented in **Fig. 3a**, it was found that 8 normal protein bands were identified in brains of healthy rats at Rfs 0.01, 0.21, 0.36, 0.48, 0.62, 0.72, 0.85 and 0.96 (B% 16.42, 12.44, 12.57, 12.64, 12.57, 10.88, 12.38 and 10.10 ; Quant. 6.60, 5.96, 5.99, 8.99, 5.99, 5.04, 8.97 and 1.98, respectively). There are 5 common protein bands identified at Rfs 0.01, 0.36, 0.62, 0.72 and 0.96 (B% 16.42, 12.57, 12.57, 10.88 and 10.10 ; Quant. 6.60, 5.99, 5.99, 5.04 and 1.98, respectively).

Silver *M. oleifera* leaves nano-extract at both doses (0.7 and 1.4 g/kg) caused no alterations at the physiological state in brains of rats. This was supported by the SI values that reached the highest level (100%). As regard to *C. tiglium* seeds extract, it was emphasized that silver *C. tiglium* seeds nano-

extract at a dose of 3.3 ml/kg caused no electrophoretic alterations in protein pattern. Furthermore, nano-extract at the dose 6.5 ml/kg caused qualitative alterations represented by hiding 3 normal bands with existence of 3 characteristic (abnormal) ones identified at Rfs 0.11, 0.27 and 0.52 (B% 12.46, 12.33 and 12.00 ; Quant. 6.76, 7.67 and 6.28, respectively). Therefore, the SI value reached the lowest value (62.5%) in this nano-extract treated group. This was in agreement with Shim *et al.* [72] who suggested that the changes in native protein pattern might be attributed to ability of the nanoparticles to react with proteins in the brain tissues. Moreover, these alterations might refer to the oxidative damage occurred as a result of abundance of brain proteins and the increased its reaction rates with a wide range of radicals and reactive species. These reactive species cause chemical changes like fragmentation, cross-linking, aggregation and oxidation in the protein molecules [76].

Lipoproteins are lipid-protein complexes. They are consisting of large insoluble glycerides and cholesterol coated superficially by phospholipids and proteins. They are responsible for carrying different proportions of all types of lipids. Therefore, there is direct proportional between density of lipoprotein to protein content and inversely proportional to lipid content [77]. During the present study, it was noticed that 6 normal lipoprotein bands were identified in healthy brain tissues at Rfs 0.14, 0.27, 0.47, 0.57, 0.69 and 0.97 (B% 18.67, 20.14, 19.14, 15.33, 15.01 and 11.71 ; Quant. 7.58, 10.54, 15.94, 4.58, 9.93 and 4.38, respectively). All control bands are common (**Fig. 3b**). Administration of silver *M. oleifera* leaves nano-extract at both doses caused no electrophoretic alterations in brains of rats when compared to control and *M. oleifera* leaves extract treated group (without Ag-NPs). The SI values reached the highest level (100%) in that nano-extracts treated groups. While in silver *C. tiglium* seeds nano-extract treated groups, it was found that presence of Ag-NPs caused no electrophoretic alterations in lipoprotein pattern when administrated at a dose of 3.3 ml/kg. Moreover, silver *C. tiglium* seeds nano-extract at a dose of 6.5 ml/kg altered lipoprotein pattern qualitatively through existence of one abnormal characteristic band identified at Rf 0.81 (B% 11.44 ; Quant. 5.00) without hiding normal ones. Therefore, the SI value decreased (92.31%) in this nano-extract treated group as compared to those (100%) of the other nano-extracts treated groups. Alterations of the lipoprotein pattern might refer to the adverse effect of ROS that exhibits oxidative modifications resulting in small lipoproteins.

Bonnefont-Rousselot [78] supported our findings and suggested that ROS initiate one-electron oxidation or one-electron reduction reactions on

numerous biological systems and the oxidative hypothesis classically admits involvement of the lipoproteins oxidation. In addition, there was natural binding between protein and lipoproteins in the brain tissues. Therefore, the abnormalities in the lipoprotein pattern might be occurred as a consequence to altering the protein pattern in that tissue. Also, lipoprotein pattern might be altered due to the disturbances in the cholesteryl esterase required or cholesterol hydrolysis [79]. It is well known that CAT and POX play an important role in detoxification of free radicals [80]. As illustrated in **Fig. 4a**, it was observed that CAT pattern was expressed electrophoretically in healthy brain tissues by 4 normal types identified at Rfs 0.37, 0.51, 0.62 and 0.95 (B% 27.19, 26.58, 24.48 and 21.74 ; Quant. 7.85, 8.77, 4.85 and 5.20, respectively). Three common CAT bands were identified at Rfs 0.37, 0.51 and 0.95 (B% 27.19, 26.58 and 21.74; Quant. 7.85, 8.77 and 5.20, respectively). No alterations occurred in electrophoretic CAT pattern of brain tissues as a result of the treatment with silver *M. oleifera* leaves non-extract at both doses. This finding was supported by the highest SI values (100%) noticed in nano-extracts at both doses. On the other hand, it was found that silver *C. tiglium* seeds nano-extract at the dose 3.3 ml/kg caused no electrophoretic alterations in CAT pattern. Moreover, administration of silver *C. tiglium* seeds nano-extract at a dose of 6.5 ml/kg caused qualitative alterations expressed by hiding the one normal CAT band without existence of abnormal ones. Therefore, the SI value decreased (85.71%) in this nano-extract treated group as compared to those (100%) of the other nano-extracts treated groups. In addition, the nano-extract at that dose caused quantitative abnormalities through decreasing quantity of the 2nd CAT band (Rf 0.49 ; B% 33.36 and Quant. 2.01).

As presented in **Fig. 4b**, it was found that POX pattern was represented electrophoretically in healthy brain tissues by 4 normal types identified at Rfs 0.04, 0.52, 0.72 and 0.77 (B% 26.66, 26.47, 23.85 and 23.02 ; Quant. 4.80, 5.42, 4.10 and 3.96, respectively). Three common POX bands were identified at Rfs 0.04, 0.72 and 0.77 (B% 26.66, 23.85 and 23.02; Quant. 4.80, 4.10 and 3.96, respectively). The electrophoretic POX pattern showed no differences in brains as a result of the treatment with silver *M. oleifera* leaves nano-extract at both doses. This finding was supported by the highest SI values (100%) noticed in nano-extracts treated at that doses. On the other hand, it was found that silver *C. tiglium* seeds nano-extract at the dose 3.3 ml/kg caused no electrophoretic alterations in POX pattern. While at a dose of 6.5 ml/kg, it caused qualitative alterations expressed by hiding the 2nd

POX band without existence of abnormal ones. Therefore, the SI value decreased (85.71%) in this nano-extract treated group as compared to those (100%) of the other nano-extracts treated groups. According to the present data, the electrophoretic CAT and POX were altered in brains of silver *C. tiglium* seeds nano-extract treated rats. This might be due to uncontrolled production of ROS and accumulation of H₂O₂ and this consequently leads to the oxidative damage as evidenced by perturbations in various antioxidant enzymes [81]. Depletion in activities of these enzymes could be due to the direct effect of ROS on the enzymes or the protein portion of these enzymes. Consequently, these ROS are able to change the physic-chemical and immunologic properties of endogenous CAT and POX enzymes [82]. In consistent to results of the present experiment, depletion in GSH level was responsible for the disturbances detected electrophoretically in POX pattern. This finding was supported by Bhatia and Manda [80] who suggested that GSH acts as a substrate for POX to catalyze reduction of organic hydroperoxides leading to elevation of H₂O₂ and hence generation of the free radicals.

Esterases are large class of the enzymes that are very polymorphic and tissue-specific. They belong to the lysosomal lipolytic enzymes that are characterized by their ability to catalyze hydrolysis of ester bonds in the neutral lipids (i.e., triglyceride and cholesterol esters) introduced into cells as components of lipoproteins and lipid deposits and break them down into the corresponding carboxylic acids [83]. The brain was selected to show the esterase activity because it is rich in esterase enzyme due to its role in the neurotransmission and communication of messages [84]. Esterases are found associated with membrane structures and they exhibit their activity through stimulating breakdown of acetylcholine liberated during nervous stimulation [85]. Electrophoresis plays a major role in identifying esterases due to presence of active thiol groups which facilitate the electrophoretic detection [73]. As illustrated in **Fig. 5a**, it was noticed that α -EST pattern was electrophoretically represented in brains of healthy rats by 2 normal types identified at Rfs 0.08 and 0.63 (B% 51.07 and 48.93; Quant. 11.34 and 10.41, respectively). The α -EST bands are considered as 2 common bands. Incorporation of Ag-NPs into *M. oleifera* leaves extract caused no abnormalities in brains of rats treated with the nano-extract at both doses. Therefore, the SI reached the highest level (100%). As regard to *C. tiglium* seeds extract, it was found that silver *C. tiglium* seeds nano-extract at a dose of 3.3 ml/kg caused no electrophoretic alterations in α -EST pattern. Furthermore, administration of silver *C. tiglium* seeds

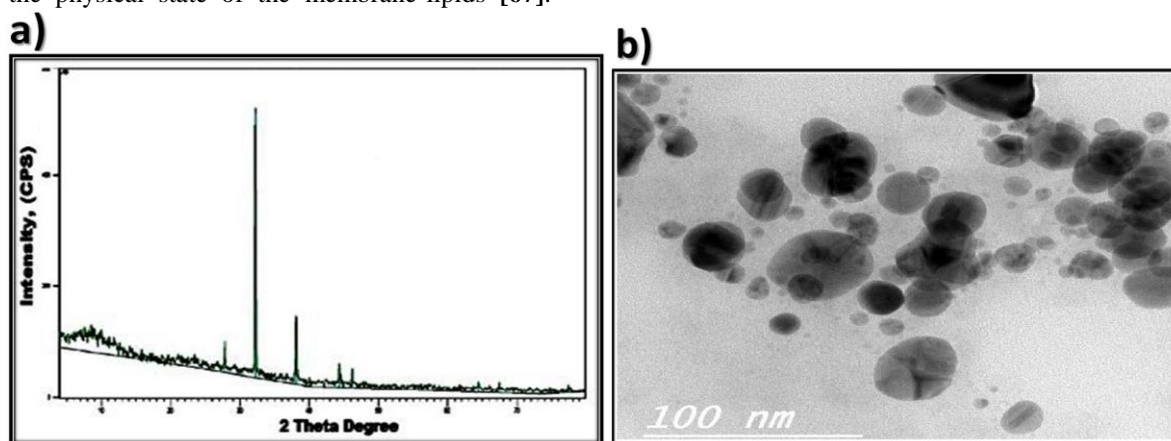
nano-extract at the dose 6.5 ml/kg caused no alterations at the qualitative level (the highest SI value (100%)). As regard to the quantitative level, it caused abnormalities represented by increased quantity of the 2nd α -EST band (Rfs 0.59; B% 50.32 and Quant. 30.07).

As presented in **Fig. 5b**, it was noticed that 5 normal β -EST bands were identified in healthy brain tissues at Rfs 0.03, 0.24, 0.65, 0.76 and 0.86 (B% 23.58, 21.50, 19.05, 18.90 and 16.97 ; Quant. 6.29, 1.72, 16.00, 11.34 and 15.38, respectively). Two common bands were identified at Rfs 0.03 and 0.86 (B% 23.58 and 16.97; Quant. 6.29 and 15.38, respectively). Incorporation of Ag-NPs into *M. oleifera* leaves extract caused no electrophoretic alterations in brains of rats treated with the nano-extract at both doses. The SI values reached the highest level (100%) in that nano-extracts treated groups. While in silver *C. tiglium* seeds nano-extract treated groups, it was observed that presence of Ag-NPs caused no electrophoretic alterations in the electrophoretic β -EST pattern when administrated at the dose 3.3 ml/kg. Moreover, administration of silver *C. tiglium* seeds nano-extract at the dose 6.5 ml/kg caused qualitative alterations represented by hiding the 2nd, 3rd and 4th normal β -EST bands with existence of 2 characteristic (abnormal) bands identified at Rf 0.03 and 0.88 (B% 28.01 and 20.22 ; Quant. 5.79 and 7.32, respectively). Therefore, the SI value reached the lowest value (44.44%) in this nano-extract treated group.

During the present study, this nano-extract caused mutagenicity detected electrophoretically in the α - and β -esterases. This might be attributed to its effect on the membrane bound enzymes that are sensitive to changes in membrane fluidity and reflects alterations in the physical state of the membrane-lipids [67].

Furthermore, these deleterious effects might occur as a result of effect of the free radicals on integrity of protein molecule through fragmentation of polypeptide chain due to sulfhydryl-mediated cross linking of the labile amino acids as claimed by Bedwell *et al.* [86]. The changes in fractional activity of the different isoenzymes seemed to be correlated with changes in rate of protein expression secondary to DNA damage initiated by these reactive species [87]. Therefore, the abnormalities detected electrophoretically in the native protein pattern might reflect alterations in the EST patterns.

As shown in **Fig. 6**, the genomic DNA in brain of control group was represented as one thick band (Rfs 0.15; Mwt 2069.57 bp; B% 89.54 and Quant. 16.11). No alterations occurred in the genomic DNA pattern of brain tissues as a result of the treatment with silver *M. oleifera* leaves non-extract at both doses as compared to control and group treated with *M. oleifera* leaves extract (without Ag-NPs). On the other hand, it was found that silver *C. tiglium* seeds nano-extract caused no alterations in the genomic DNA pattern when administrated at a dose of 3.3 ml/kg. The dose 6.5 ml/kg of *C. tiglium* nano-extract enhanced cleavage of the genomic DNA leading to 4 bands (Rfs 0.13, 0.51, 0.67 and 0.93 ; Mwts 2102.50, 1200.00, 1022.76 and 787.79 bp ; B% 20.52, 24.50, 26.05 and 28.93 ; Quant. 3.00, 8.58, 1.78 and 7.32, respectively). This was in accordance with Milligan and Ward [88] who reported that the DNA cleavages attributed to attack of the \cdot OH radicals that targeting purine and pyrimidine bases and able to react easily with deoxyribose. Moreover, they are able to interact with double bonds and / or to extract hydrogen atoms from nucleic acids leading to DNA damage.



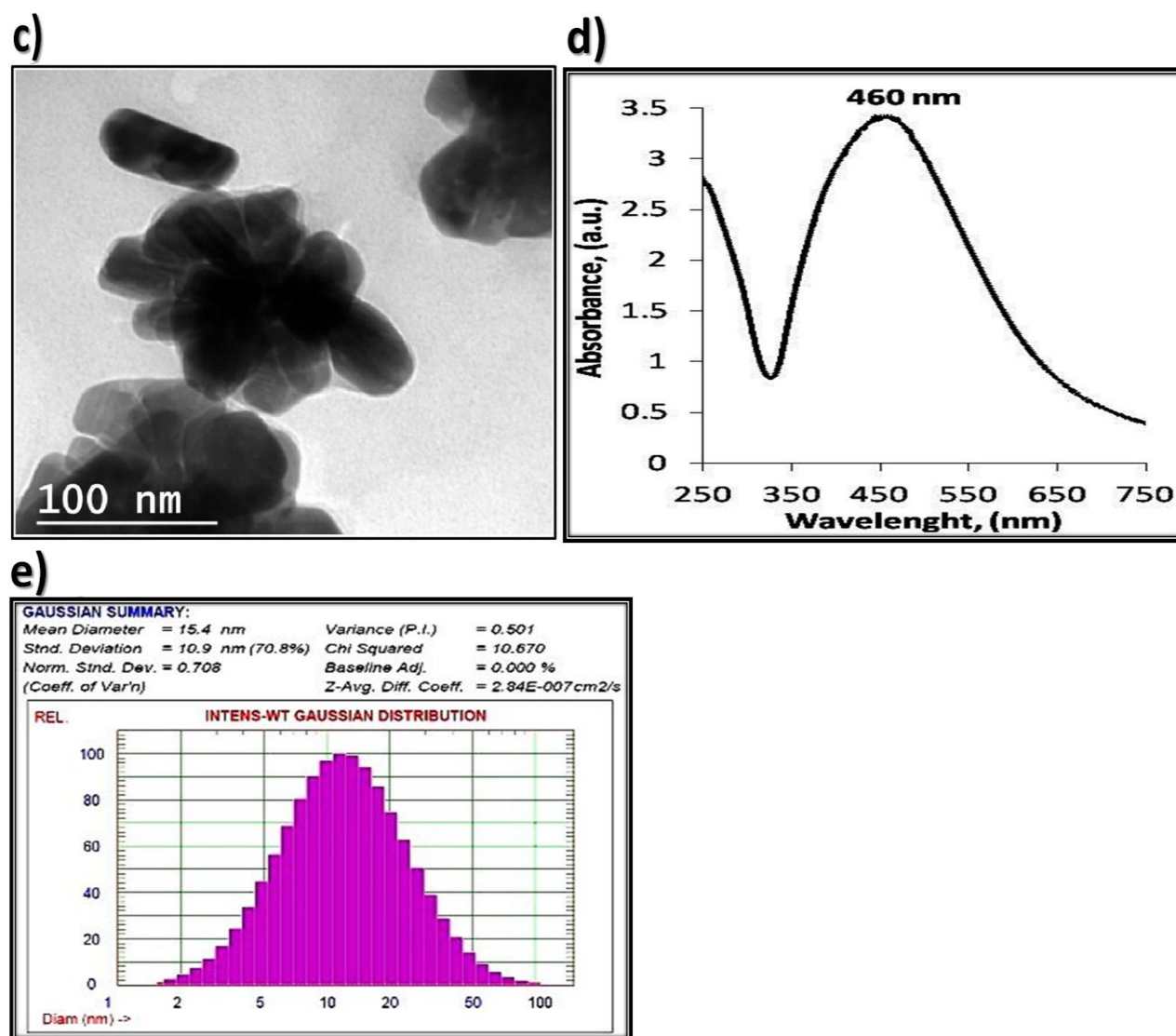


Fig. 1. Characterization of the synthesized silver nanoparticles (Ag-NPs) showing **a)** X-Ray Diffraction (XRD) pattern, **b)** Transmission Electron Microscope (TEM) image of Ag-NPs incorporated into *C. tiglium* seeds extract, **c)** TEM image of Ag-NPs incorporated into *M. oleifera* leaves extract, **d)** Ultraviolet-visible (UV-VIS) spectroscopy and **e)** Dynamic Light Scattering (DLS)

TABLE 1. Effect of *C. tiglium* seeds and *M. oleifera* leaves extracts and their silver nano-extracts on levels of oxidative stress non-enzymatic markers in rats' brain tissues

C.	C. t	Silver <i>C. tiglium</i> seeds nano-extract		M. o	Silver <i>M. oleifera</i> leaves nano-extract		
		3.3 ml/kg	6.5 ml/kg		0.7 g/kg	1.4 g/kg	
LPO (nmol/g)	312.96 ± 2.55	312.95 ± 2.79	313.68 ± 2.95	820.03 ^{ab} ± 4.05	314.97 ± 3.41	313.24 ± 2.96	314.52 ± 2.85
TAC (µmol/g)	27.43 ± 0.20	27.22 ± 0.32	27.40 ± 0.21	8.64 ^{ab} ± 0.03	27.23 ± 0.27	27.17 ± 0.17	27.43 ± 0.23
GSH (mmol/g)	8.58 ± 0.04	8.57 ± 0.05	8.55 ± 0.04	5.62 ^{ab} ± 0.04	8.55 ± 0.04	8.63 ± 0.03	8.68 ± 0.01
Nitrite (nmol/g)	40.43 ± 0.48	41.14 ± 0.80	41.96 ± 0.21	70.83 ^{ab} ± 0.38	40.85 ± 0.48	40.68 ± 0.75	40.82 ± 0.56

C.: Control; C. t: *Croton tiglium*; M. o: *Moringa oleifera*

"a" indicated significant difference (P<0.05) as compared to control group, "b" indicated significant difference (P<0.05) as compared to *C. tiglium* seeds extract treated group.

TABLE 2. Effect of *C. tiglium* seeds and *M. oleifera* leaves extracts and their silver nano-extracts on activities of antioxidant enzymes in brain tissues of rats

C.	C. t	Silver <i>C. tiglium</i> seeds nano-extract		M. o	Silver <i>M. oleifera</i> leaves nano-extract		
		3.3 ml/kg	6.5 ml/kg		0.7 g/kg	1.4 g/kg	
SOD (U/g)	11.42 ± 0.01	11.42 ± 0.01	11.40 ± 0.03	5.22 ^{ab} ± 0.02	11.40 ± 0.02	11.41 ± 0.01	11.42 ± 0.01
CAT (U/g)	6.65 ± 0.05	6.66 ± 0.05	6.66 ± 0.06	4.04 ^{ab} ± 0.19	6.65 ± 0.06	6.66 ± 0.05	6.64 ± 0.06
Gpx (U/g)	5.26 ± 0.02	5.22 ± 0.03	5.22 ± 0.03	2.73 ^{ab} ± 0.03	5.28 ± 0.03	5.27 ± 0.02	5.28 ± 0.01

C.: Control; C. t: *Croton tiglium*; M. o: *Moringa oleifera*

"a" indicated significant difference (P<0.05) as compared to control group, "b" indicated significant difference (P<0.05) as compared to *C. tiglium* seeds extract treated group.

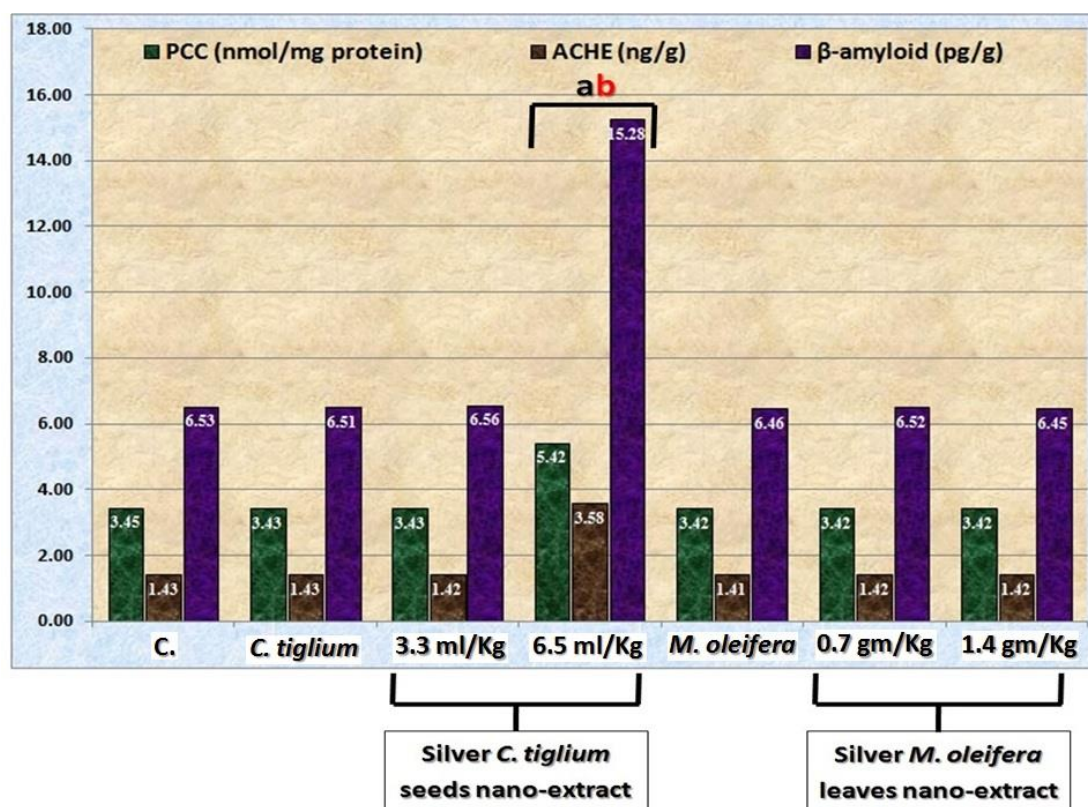


Fig. 2. Effect of *C. tiglium* seeds and *M. oleifera* leaves extracts and their silver nano-extracts on protein carbonyl content (PCC), acetylcholine esterase (ACHE) and β -amyloid ($A\beta$) content in brain tissues of rats.

"a" indicated significant difference ($P < 0.05$) as compared to control group, "b" indicated significant difference ($P < 0.05$) as compared to *C. tiglium* seeds extract treated group.

TABLE 3. Effect of *C. tiglium* seeds and *M. oleifera* leaves extracts and their silver nano-extracts on inflammatory markers (interleukin- 1β and tumor necrosis factor- α) in rats' brain tissues

	C.	<i>C. t</i>	Silver <i>C. tiglium</i> seeds nano-extract		<i>M. o</i>	Silver <i>M. oleifera</i> leaves nano-extract	
			3.3 ml/kg	6.5 ml/kg		0.7 g/kg	1.4 g/kg
IL-1β (pg/g)	449.14 ± 1.06	453.43 ± 1.17	452.71 ± 0.89	767.71 ^{ab} ± 1.55	452.14 ± 0.83	454.14 ± 1.59	452.00 ± 1.20
TNF-α (pg/g)	120.43 ± 1.15	121.00 ± 0.87	120.86 ± 0.77	168.86 ^{ab} ± 1.18	121.86 ± 1.33	121.00 ± 1.15	121.00 ± 1.27

C.: Control; *C. t*: *Croton tiglium*; *M. o*: *Moringa oleifera*

"a" indicated significant difference ($P < 0.05$) as compared to control group, "b" indicated significant difference ($P < 0.05$) as compared to *C. tiglium* seeds extract treated group.

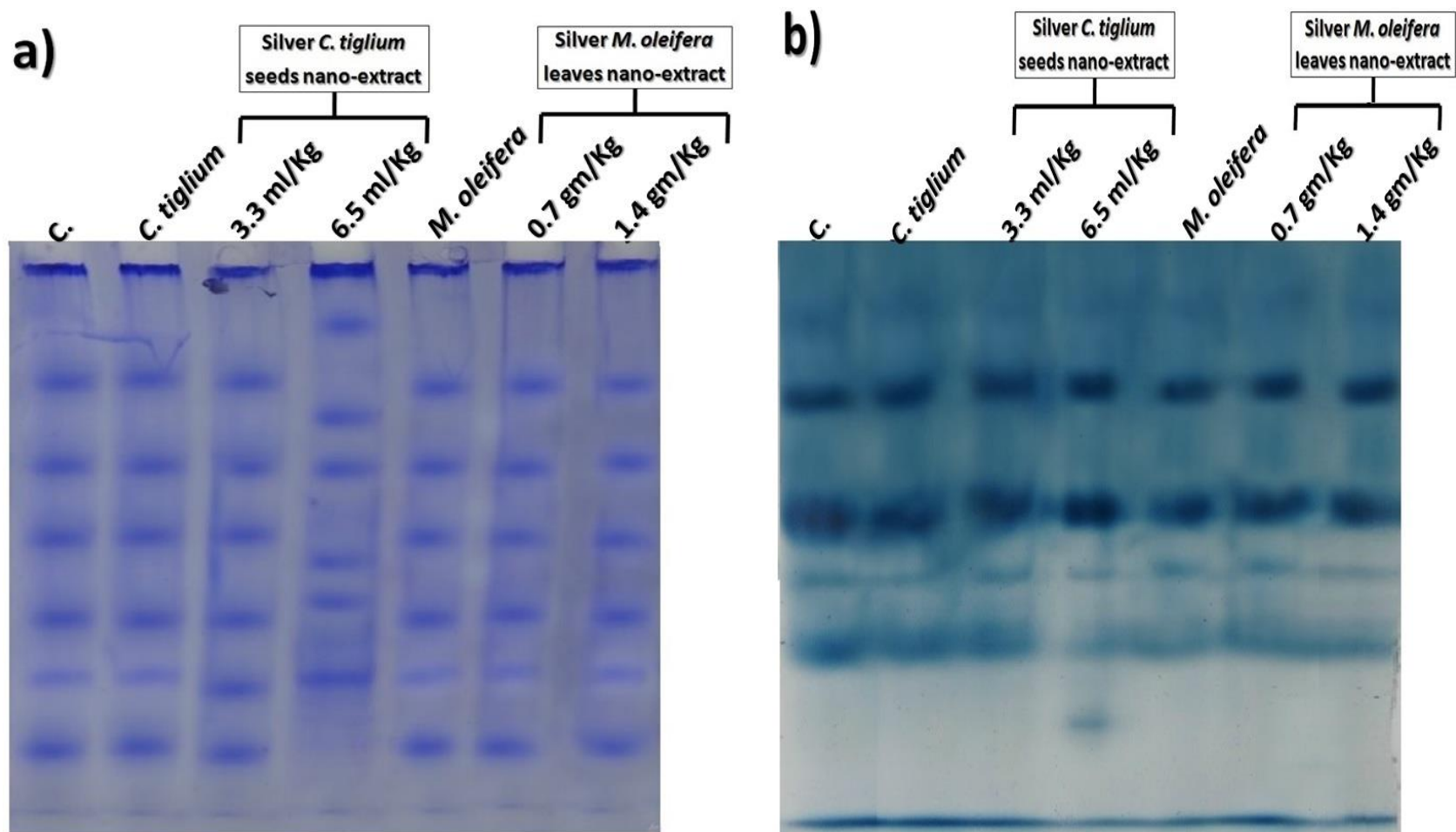


Fig. 3. Electrophoretic patterns illustrating of *C. tiglium* seeds and *M. oleifera* leaves extracts and their silver nano-extracts on a) native protein and b) lipid moiety of native protein in rats' brain tissues.

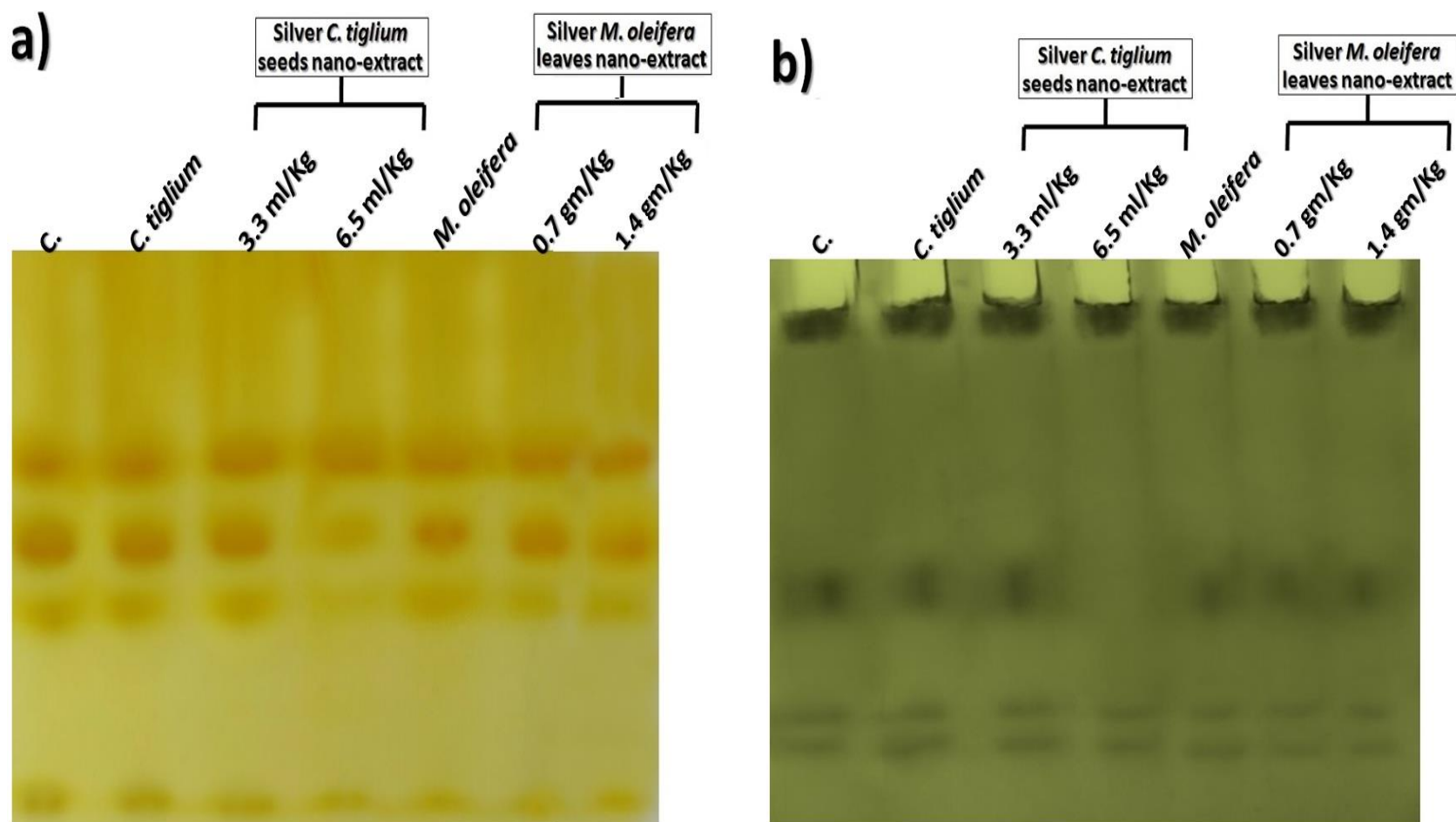


Fig. 4. Electrophoretic isozymes revealing effect of *C. tiglium* seeds and *M. oleifera* leaves extracts and their silver nano-extracts on **a)** catalase (CAT) pattern and **b)** peroxidase (POX) pattern in rats' brain tissues.

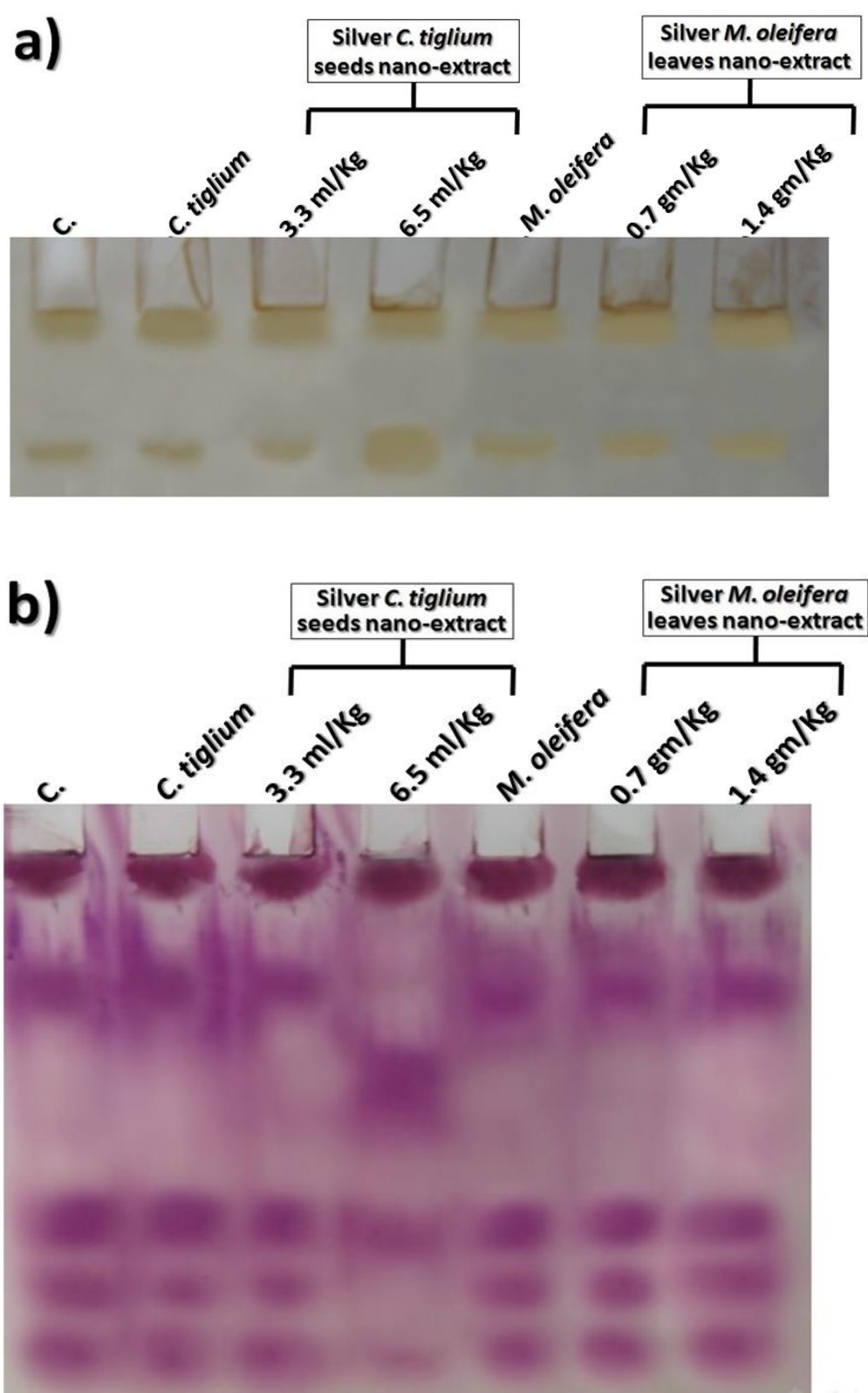


Fig. 5. Electrophoretic isozymes showing effect of *C. tiglium* seeds and *M. oleifera* leaves extracts and their silver nano-extracts on **a)** α -esterase (α -EST) pattern and **b)** β -esterase (β -EST) pattern in murine brain tissues.

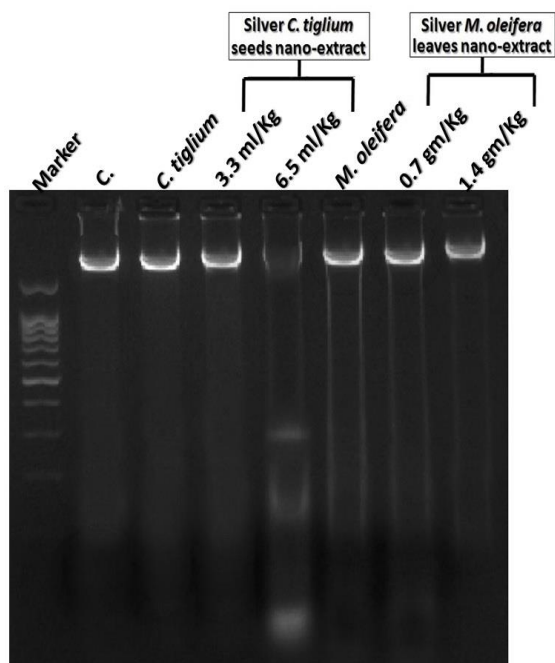


Fig. 6. Genomic DNA pattern showing effect of *C. tiglium* seeds and *M. oleifera* leaves extracts and their silver nano-extracts on DNA integrity in brain tissues of rats.

Furthermore, mechanism of the repair activity impaired due to accumulation of the radicals leading to severe oxidative DNA damage [89]. BLAST and FASTA comparative analysis gave similarity percentage of 49.00 ± 0.15 between the query and templates sequences which is consider a good alignment (acceptable similarity is $> 20\%$) [75]. Secondary structure analysis showed that the sequence consisted of dominant flexible coil and sheet regions with minor rigid helix part allocated at region 129~148. Threading process using TASSER was performed using top 5 alignment homologs, using their X-ray crystallographic structures from the PDB database as templates (Fig. 7).

Based in this analysis, 3D models were constructed had C-score range $-1.83 \sim 4.19$, the highest C-score ($= -1.85$) model was picked up for refinement. Refinement step gave a high-quality model as can be seen in Fig. 8a. Ramachandran plot analysis was done for both original and refine models to ensure the modelling validity. Initial model showed 62.2, 22.4 and 15.4% residues located in favoured, allowed and outlier regions,

respectively, while in the refine model the ratios were 83.3, 14.1, and 2.6% of residues in the same regions (Figs. 8b&c).

As seen from the constructed model, coils represent the major parts giving an indication of the high flexibility of the regions. These results suggested relative law stability with expectation of high reactivity of the protein under investigation [90]. To find the most reactive region that represent weak sites of INF- γ protein, surface analysis using sphere generating algorithm was done on the refined model. According to this analysis the residues range 119~127 represent the most reactive site. The high flexibility of this site is not the only reason of the high reactivity, but also the lake of hydrogen bonding network between the residues in this region (Fig. 9).

4. Conclusion

The study concluded that silver *M. oleifera* leaves nano-extract at both studied doses (0.7 and 1.4 g/kg) caused no significant alterations in all biochemical measurements or electrophoretic patterns in brain tissues. Silver *C. tiglium* seeds nano-extract caused no significant differences when administrated at a dose of 3.3 ml/kg. While at a dose of 6.5 ml/kg, it increased ACHE, A β contents, LPO, PCC, nitrite and inflammatory markers (IL-1 β and TNF- α) significantly ($P < 0.05$) associated with lowering TAC, GSH, SOD, CAT and Gpx levels in brain tissues. Furthermore, it caused qualitative abnormalities represented electrophoretically from the differences in arrangement of the native bands. Therefore, nano-extract treated group at a dose of 6.5 ml/kg was noticed with lower SI values (62.5, 92.31, 85.71, 85.71 and 44.44%; native protein, lipid moiety of protein, CAT, POX and β -EST, respectively). It caused quantitative abnormalities in the α -EST pattern through variations in quantity of 2nd α -EST band. In addition, it enhanced DNA cleavage giving 4 bands. Moreover, the molecular dynamic simulation showed that the residues range 119~127 represent the most reactive and flexible site in the INF- γ receptor protein.

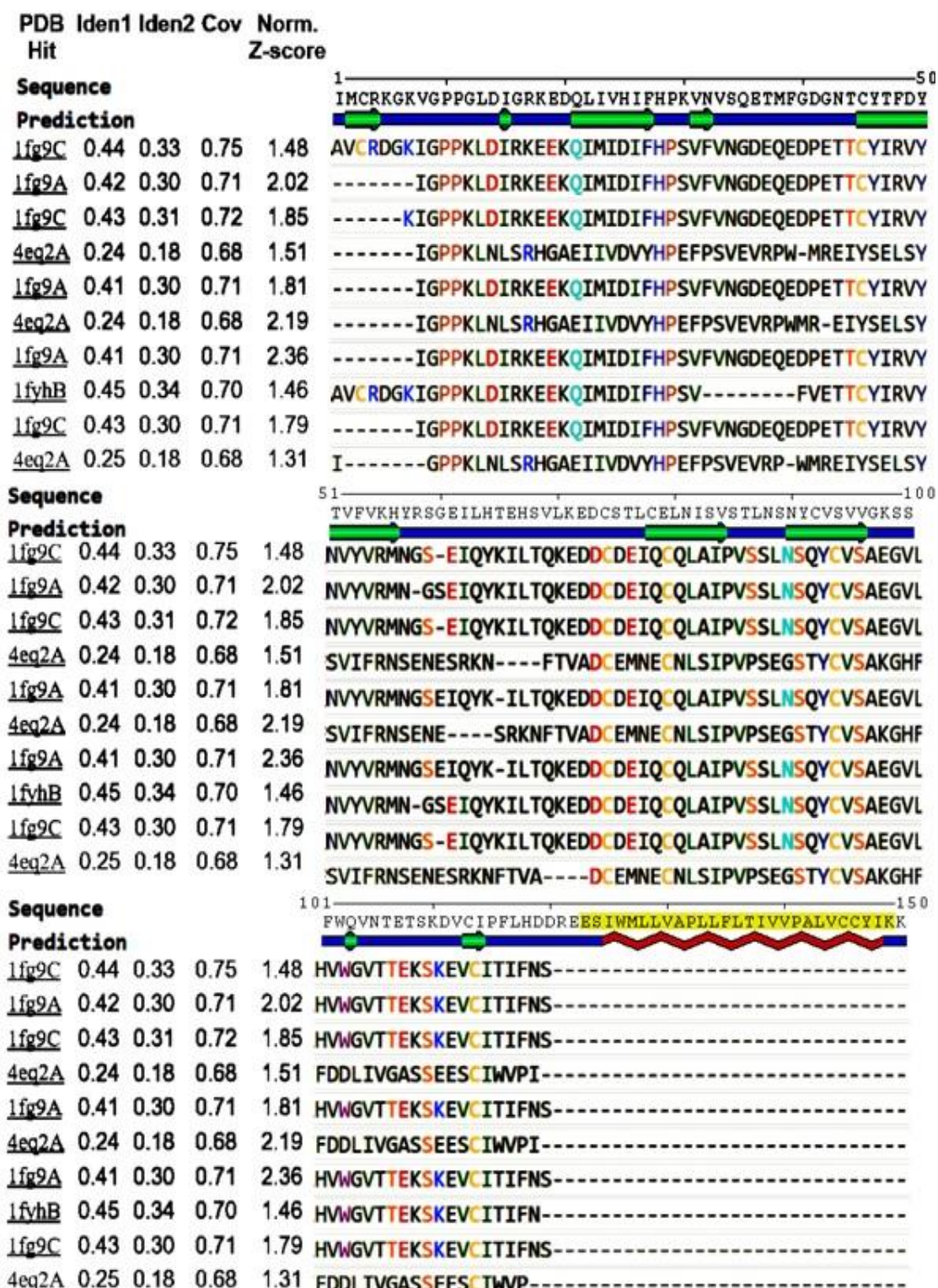


Fig. 7. Sequence alignments of INF- γ protein receptor and its homolog structures extracted from the protein data bank (PDB) database. Colored prediction represents coil (blue), sheet (green) and helix (red). Amino acids are colored based on their properties.

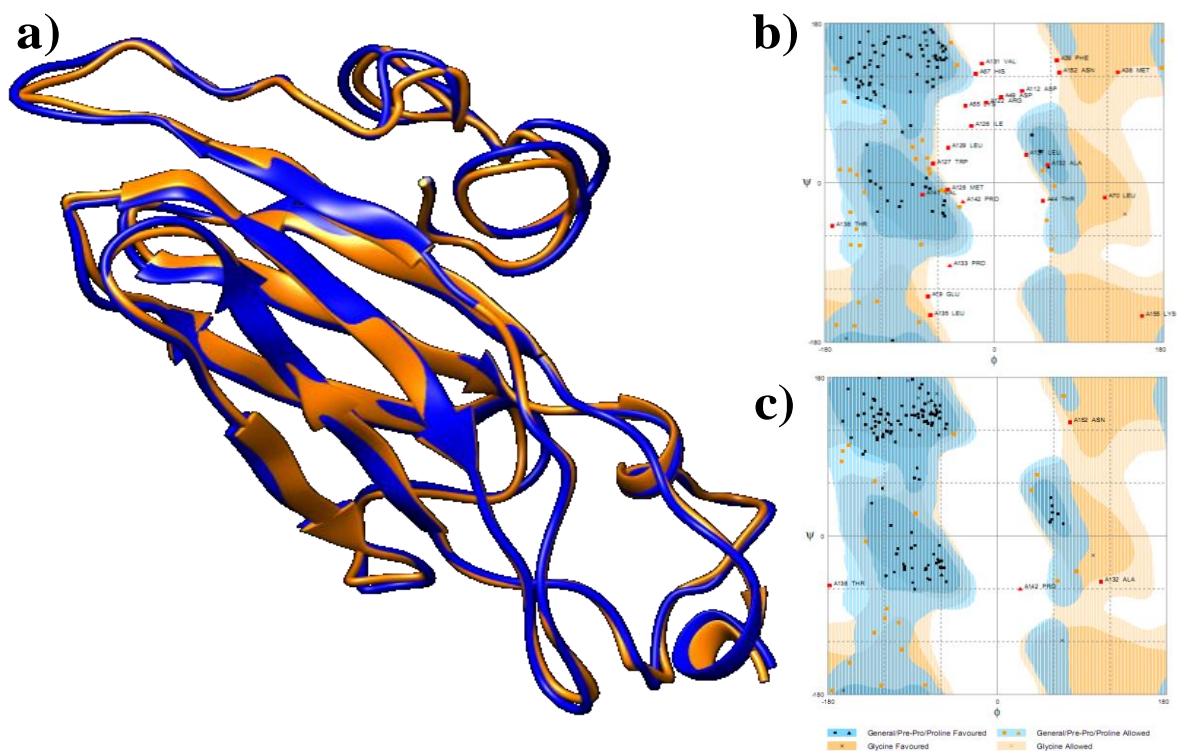


Fig. 8. a) 3D refined INF- γ receptor protein (dark blue) Superimposed to the initial constructed model (orange), b) and c) are colored representation Ramachandran plots for the initial and refined models, respectively.

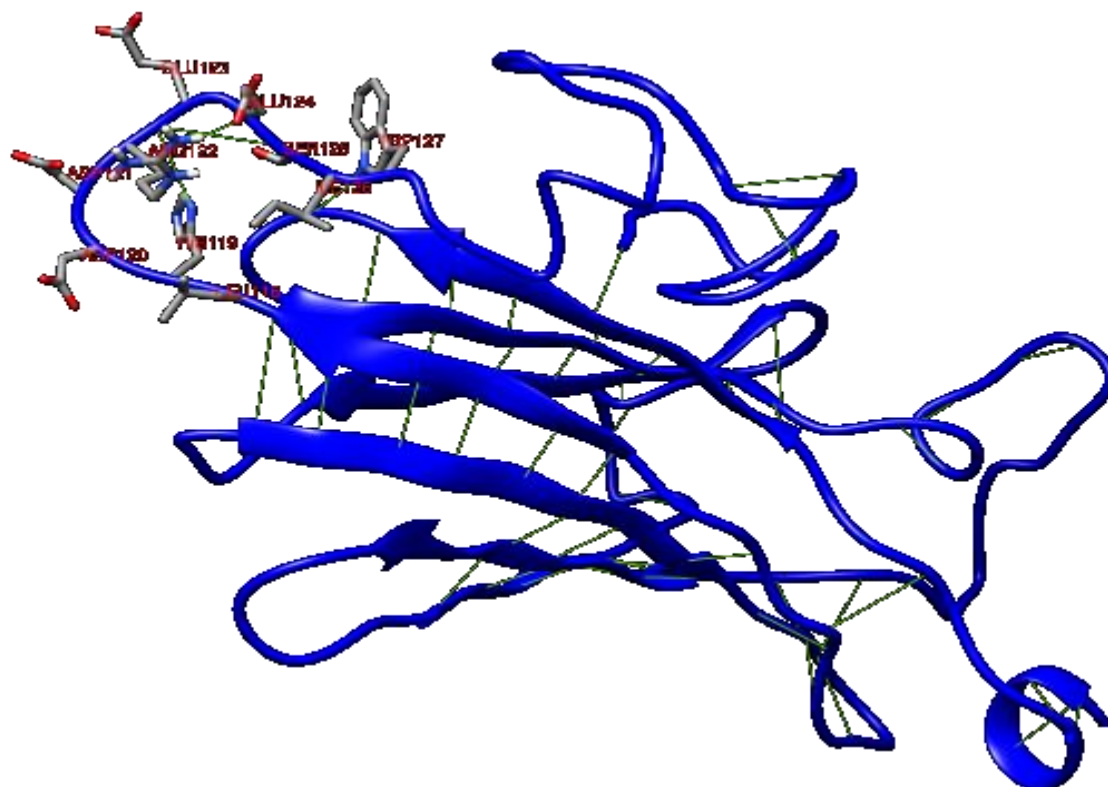


Fig. 9. Most reactive region (LEU118, HIS119, ASP120, ASP121, ARG122, GLU123, GLU124, SER125, ILE126, and TRP127) of INF- γ protein generated using sphere generating algorithm with H-bonds network as green lines.

5. Author Contributions

WMA, RKS and NIO suggested the idea and collected all papers published previously and related to that idea. Also, they put the practical plan. MMS and HAE helped for carrying out the practical work on experimental animals. AMY was concerned with preparing silver plant nano-extracts. WMA, MI and NMO were responsible for carrying out molecular work as well as dynamic modelling and simulation. All authors read and approved the final form of manuscript.

6. Funding Statement

None

7. Conflict of Interests

The authors who are responsible for the manuscript theoretically and practically have no declared conflicts of financial and non-financial interests.

8. References

- Nath, R.; Roy, S. ; De, B. and Choudhury, M.D. Anticancer and antioxidant activity of croton: A review. *International Journal of Pharmacy and Pharmaceutical Sciences*, **5**, 63-70 (2013).
- Hecker, E. Cocarcinogenic principles from the seed oil of *Croton tiglium* and from other Euphorbiaceae. *Cancer Res.*, **28**, 2338-2349 (1968).
- Sengul, M. ; Yildiz, H. ; Gungor, N. ; Cetin, B. ; Eser, Z. and Ercisli, S. Total phenolics content, antioxidant and antimicrobial activities of some medicinal plants. *Pak. J. Pharm. Sci.*, **22**, 102-106 (2009).
- Hu, J. ; Gao, W.Y. ; Gao, Y. ; Ling, N.S. ; Huang, L.Q. and Liu, C.X. M3 muscarinic receptor- and Ca²⁺ influx-mediated muscle contractions induced by croton oil in isolated rabbit jejunum. *J. Ethnopharmacol.*, **129**, 377-380 (2010).
- Rickard, K.L. ; Gibson, P.R. ; Young, G.P. and Phillips, W.A. Activation of protein kinase C augments butyrate induced differentiation and turnover in human colonic epithelial cells *in vitro*. *Carcinogenesis* (Lond.), **20**, 977-984 (1999).
- El-Kamali, H.H. ; Omran, A.M.E. and Abdalla, M.A. Biochemical and haematological assessment of *Croton tiglium* seeds mixed with animal diet in male albino rats. *Annual Research & Review in Biology*, **8**, 1-7 (2015).
- Jahn, S.A. Using Moringa seeds as coagulant in developing countries. *J. Am. Works Assoc.*, **80**, 43-50 (1988).
- Mohamed, F.A., Salama, H.H., El-Sayed, S.M., El-Sayed, H.S. and Zahran, H.A. Utilization of natural antimicrobial and antioxidant of Moringa oleifera leaves extract in manufacture of cream cheese. *J Biol Sci*, **18**(2), pp.92-106. (2018).
- El-Naggar, M.E., Hussein, J., El-sayed, S.M., Youssef, A.M., El Bana, M., Latif, Y.A. and Medhat, D. Protective effect of the functional yogurt based on Malva parviflora leaves extract nanoemulsion on acetic acid-induced ulcerative colitis in rats. *Journal of Materials Research and Technology*, **9**(6), 14500-14508 (2020).
- Berkovich, L. ; Earon, G. ; Ron, I. ; Rimmon, A. ; Vexler, A. and Lev-Ari, S. *Moringa oleifera* aqueous leaf extract down-regulates nuclear factor-kappa Band increases cytotoxic effect of chemotherapy in pancreatic cancer cells, BMC Complement. *Altern. Med.*, **13**, 212-219 (2013).
- Kirisattayakul, W. ; Wattanathorn, J. ; Tong-Un, T. ; Muchimapura, S. ; Wannanon, P. and Jittiwat, J. Cerebroprotective Effect of against Focal Ischemic Stroke Induced by Middle Cerebral Artery Occlusion. *Hindawi Publishing Corporation, Oxidative Medicine and Cellular Longevity*, Article ID 951415, 10 pages (2013).
- Leone, A. ; Spada, A. ; Battezzati, A. ; Schiraldi, A. ; Aristil, J. and Bertoli, S. Cultivation, Genetic, Ethnopharmacology, Phytochemistry and Pharmacology of *Moringa oleifera* Leaves: An Overview. *International journal of molecular sciences*, **16**, 12791-12835 (2015).
- Aboulthana, W.M., Ibrahim, N.E.S., Osman, N.M., Seif, M.M., Hassan, A.K., Youssef, A.M., El-Feky, A.M. and Madboli, A.A. Evaluation of the Biological Efficiency of Silver Nanoparticles Biosynthesized Using *Croton tiglium* L. Seeds Extract against Azoxymethane Induced Colon Cancer in Rats. *Asian Pacific Journal of Cancer Prevention: APJCP*, **21**(5), p.1369. (2020).
- Saada, N.S., Abdel-Maksoud, G., Abd El-Aziz, M.S. and Youssef, A.M., 2021. Green synthesis of silver nanoparticles, characterization, and use for sustainable preservation of historical parchment against microbial

- biodegradation. *Biocatalysis and Agricultural Biotechnology*, **32**, 101948 (2021)
15. El-Sayed, S.M., El-Naggar, M.E., Hussein, J., Medhat, D. and El-Banna, M. Effect of *Ficus carica* L. leaves extract loaded gold nanoparticles against cisplatin-induced acute kidney injury. *Colloids and Surfaces B: Biointerfaces*, **184**, p.110465 (2019).
 16. Mohanpuria, P. ; Rana, N.K. and Yadav, S.K. Biosynthesis of nanoparticles: technological concepts and future applications. *J. Nanoparticle Res.*, **10**, 507-517 (2008).
 17. Hanaa, D., Youssef, A., El-Metwally, E. and Abdelaal, M. Preparation and Characterization of Novel Poly (MMA-co-GMA)/Ag Nanocomposites for Biomedical Applications. *Egyptian Journal of Chemistry*, **62**(12), pp.2245-2252. (2019).
 18. De Jong, W.H. ; Hagens, W.I. ; Krystek, P. ; Burger, M.C. ; Sips, A.J. and Geertsma, R.E. Particle size-dependent organ distribution of gold nanoparticles after intravenous administration. *Biomaterials*, **29**, 1912-1919 (2008).
 19. Robertson, B. ; Kong, G. ; Peng, Z. ; Bentivoglio, M. and Kristensson, K. Interferon-gamma-responsive neuronal sites in the normal rat brain: receptor protein distribution and cell activation revealed by Fos induction. *Brain Res. Bull.*, **52**, 61-74 (2000).
 20. Chesler, D.A. and Reiss, C.S. The role of IFN-gamma in immune responses to viral infections of the central nervous system. *Cytokine Growth Factor Rev.*, **13**, 441-454 (2002).
 21. Gonzalez, J.M. ; Bergmann, C.C. ; Fuss, B. ; Hinton, D.R. ; Kangas, C. ; Macklin, W.B. and Stohlman, S.A. Expression of a Dominant Negative INF- γ Receptor on Mouse Oligodendrocytes. *GLIA*, **51**, 22-34 (2005).
 22. Schroder, K. ; Hertzog, P.J. ; Ravasi, T. and Hume, D.A. Interferon-gamma: an overview of signals, mechanisms and functions. *J. Leukoc. Biol.*, **75**, 163-189 (2004).
 23. Aboulthana, W.M. ; Youssef, A.M. ; El-Feky, A.M. ; Ibrahim, N.E. ; Seif, M.M. and Hassan, A.K. Evaluation of Antioxidant Efficiency of *Croton tiglium* L. Seeds Extracts after Incorporating Silver Nanoparticles. *Egyptian Journal of Chemistry*, **62**, 181-200 (2019).
 24. Shousha, W.G. ; Aboulthana, W.M. ; Salama, A.H. ; Saleh, M.H. and Essawy, E.A. Evaluation of the biological activity of *Moringa oleifera* leaves extract after incorporating silver nanoparticles, in vitro study. *Bulletin of the National Research Centre*, **43**, 212 (2019).
 25. Levine, R.L. ; Williams, J.A. ; Stadtman, E.R. and Shacter, E. Carbonyl assays for determination of oxidatively modified proteins. *Methods Enzymol.*, **233**, 346-357 (1994).
 26. Ohkawa, H. ; Ohishi, N. and Yagi, K. Assay for lipid peroxides in animal tissues by thiobarbituric acid reaction. *Anal. Biochem.*, **95**, 351-358 (1979).
 27. Green, L.; Wagner, D. ; Glogowski, J. ; Skipper, P. ; Wishnok, J. and Tannenbaum, S. Analysis of nitrate, nitrite and [15N] nitrate in biological fluids. *Anal. Biochem.*, **126**, 131-138 (1982).
 28. Koracevic, D. ; Koracevic, G. ; Djordjevic, V. ; Andrejevic, S. and Cosic, V. Method for the measurement of antioxidant activity in human fluids. *J. Clin. Pathol.*, **154**, 356-361 (2001).
 29. Nishikimi, M. ; Rao, N.A. and Yagi, K. The occurrence of superoxide anion in the reaction of reduced phenazine methosulphate and molecular oxygen. *Biochem. Biophys. Res. Comm.*, **46**, 849-864 (1972).
 30. Aebi, H. Catalase *in vitro*. *Methods Enzymol.*, **105**, 121-126 (1984).
 31. Paglia, D.E. and Valentine, W.N. Studies on the quantitative and qualitative characterization of erythrocyte glutathione peroxidase. *The Journal of Laboratory and Clinical Medicine*, **70**, 158-163 (1967).
 32. Beutler, E. ; Duron, O. and Kelly, B.M. Improved method for the determination of blood glutathione. *J. Lab. Clin. Med.*, **61**, 882-888 (1963).
 33. March, C.J. ; Mosley, B. ; Larsen, A. ; Cerretti, D.P. ; Braedt, G. ; Price, V. ; Gillis, S. ; Henney, C.S. ; Kronheim, S.R. and Grabstein, K. Cloning, sequence and expression of two distinct human interleukin-1 complementary DNAs. *Nature*, **315**, 641-647 (1985).
 34. Engelmann, H. ; Novick, D. and Wallach, D. Two tumor necrosis factor-binding proteins purified from human urine. Evidence for immunological cross-reactivity with cell surface

- tumor necrosis factor receptors. *J. Biol. Chem.*, **265**, 1531-1563 (1990).
35. Bradford, M.M. A rapid and sensitive method for the quantitation of microgram quantities of protein utilizing the principle of protein-dye binding. *Analytical Biochemistry*, **72**, 248-254 (1976).
36. Laemmli, U.K. Cleavage of structural proteins during the assembly of the head of Bacteriophage T4. *Nature*, **227**, 680-685 (1970).
37. Darwesh, O.M. ; Moawad, H. ; Barakat, O.S. and Abd El-Rahim, W.M. Bioremediation of textile reactive blue azo dye residues using nanobiotechnology approaches. *Research Journal of Pharmaceutical Biological and Chemical Sciences*, **6**, 1202-1211 (2015).
38. Subramaniam, H.N. and Chaubal, K.A. Evaluation of intracellular lipids by standardized staining with a Sudan black B fraction. *Journal of biochemical and biophysical methods*, **21**, 9-16 (1990).
39. Siciliano, M.J. and Shaw, C.R. Separation and visualization of enzymes on gels. In 'Chromatographic and Electrophoretic Techniques. Vol. 2. Zone Electrophoresis'. 4th Edn.(Ed. I. Smith.) pp. 185-209 (1976).
40. Rescigno, A. ; Sanjust, E. ; Montanari, L. ; Sollai, F. ; Soddu, G. ; Rinaldi, A.C. ; Oliva, S. and Rinaldi, A. Detection of laccase, peroxidase, and polyphenol oxidase on a single polyacrylamide gel electrophoresis. *Anal. Lett.*, **30**, 2211-2220 (1997).
41. Ahmad, A. ; Maheshwari, V. ; Ahmad, A. ; Saleem, R. and Ahmad, R. Observation of esterase-like-albumin activity during N'-nitrosodimethyl amine induced hepatic fibrosis in a mammalian model. *Maced. J. Med. Sci.*, **5**, 55-61 (2012).
42. Barker, D.L. ; Hansen, M.S. ; Faruqi, A.F. ; Giannola, D. ; Irsula, O.R. ; Lasken, R.S. ; Latterich, M. ; Makarov, V. ; Oliphant, A. and Pinter, J.H. Two Methods of Whole-Genome Amplification Enable Accurate Genotyping Across a 2320-SNP Linkage Panel. *Genome Res.*, **14**, 901-907 (2004).
43. Porollo, A. ; Adamczak, R. and Meller, J. POLYVIEW: A Flexible Visualization Tool for Structural and Functional Annotations of Proteins. *Bioinformatics*, **20**, 2460-2462 (2004).
44. Morgulis, A. ; Coulouris, G. ; Raytselis, Y. ; Madden, T.L. ; Agarwala, R. and Schäffer, A.A. Database indexing for production Mega BLAST searches. *Bioinformatics*, **24**, 1757-1764 (2008).
45. McWilliam, H. ; Li, W. ; Uludag, M. ; Squizzato, S. ; Park, Y.M. ; Buso, N. ; Cowley, A.P. and Lopez, R. Analysis Tool Web Services from the EMBL-EBI. *Nucleic Acids Research*, **41**, W597-600 (2013).
46. Roy, A. ; Yang, J. and Zhang, Y. COFACTOR: an accurate comparative algorithm for structure-based protein function annotation. *Nucleic Acids Research*, **40**, W471-W477 (2012).
47. Yang, J. and Zhang, Y. I-TASSER server: new development for protein structure and function predictions. *Nucleic Acids Research*, **43**, W174-W181 (2015).
48. Heo, L. ; Park, H. and Seok, C. GalaxyRefine: protein structure refinement driven by side-chain repacking. *Nucleic Acids Res.*, **41**, W384-W388 (2013).
49. Popescu, M. ; Velea, A. and Lorinczi, A. Biogenic production of nanoparticles. *Dig. J. Nanomat. Bios.*, **5**, 1035-1040 (2010).
50. Aboulthana, W.M. and Sayed, H.H. How to use Green Technology to Enhance Antioxidant Efficiency of Plant Extracts: A Novel Strategy. *Journal of Applied Pharmacy*, **10**, 264-267 (2018).
51. Abdelhady, N.M. and Badr, K.A. Comparative study of phenolic content, antioxidant potentials and cytotoxic activity of the crude and green synthesized silver nanoparticles' extracts of two Phlomis species growing in Egypt. *Journal of Pharmacognosy and Phytochemistry*, **5**, 377-383 (2016).
52. Allafchian, A.R. ; Zare, M.S.Z. ; Jalali, S.A.H. ; Hashemi, S.S. and Vahabi, M.R. Green synthesis of silver nanoparticles using Phlomis leaf extract and investigation of their antibacterial activity. *J. Nanostruct. Chem.*, **6**, 129-135 (2016).
53. Youssef, A.M., Hasanin, M.S., Abd El-Aziz, M.E. and Turky, G.M. Conducting chitosan/hydroxylethyl cellulose/polyaniline bionanocomposites hydrogel based on graphene oxide doped with Ag-NPs. *International Journal of Biological Macromolecules*, **167**, pp.1435-1444. (2021).

54. Youssef, A.M., Abdel-Aziz, M.S. and El-Sayed, S.M. Chitosan nanocomposite films based on Ag-NP and Au-NP biosynthesis by *Bacillus subtilis* as packaging materials. *International journal of biological macromolecules*, **69**, pp.185-191., (2014).
55. Tang, J. ; Xiong, L. ; Wang, S. ; Wang, J. ; Liu, L. ; Li, J. ; Yuan, F. and Xi, T. Distribution, translocation and accumulation of silver nanoparticles in rats. *J. Nanosci. Nanotechnol.*, **9**, 4924-4932 (2009).
56. Ahmed, H.H. ; Shousha, W.G. ; Hussein, R.M. and Farrag, A.H. Potential role of some nutraceuticals in the regression of Alzheimer's disease in an experimental animal model. *Turk. J. Med. Sci.*, **41**, 455-466 (2011).
57. Holmquist, L. ; Stuchbury, G. ; Berbaum, K. ; Muscat, S. ; Young, S. ; Hager, K. ; Engel, J. and Münch, G. Lipoic acid as a novel treatment for Alzheimer's disease and related dementias. *Pharmacol. Ther.*, **113**, 154-164 (2007).
58. Fedorova, M. ; Kuleva, N. and Hoffmann, R. Identification, quantification, and functional aspects of skeletal muscle protein carbonylation *in vivo* during acute oxidative stress. *J. Proteome Res.*, **9**, 2516-2526 (2010).
59. Pandey, K.B. and Rizvi, S.I. Markers of oxidative stress in erythrocytes and plasma during aging in humans. *Oxidative medicine and cellular longevity*, **3**, 2-12 (2010).
60. Ishrat, T. ; Khan, M.B. ; Hoda, M.N. ; Yousuf, S. ; Ahmad, M. ; Ansari, M.A. ; Ahmad, A.S. and Islam, F. Coenzyme Q10 modulates cognitive impairment against intracerebroventricular injection of streptozotocin in rats. *Behav. Brain Res.*, **171**, 9-16 (2006).
61. Aksenov, M.Y. ; Aksenova, M.V. ; Butterfield, D.A. ; Geddes, J.W. and Markesbery, W.R. Protein oxidation in the brain in Alzheimer's disease. *Neuroscience*, **103**, 373-383 (2001).
62. Foster, K.A. ; Galeffi, F. ; Gerich, F.J. ; Turner, D.A. and Muller, M. Optical and pharmacological tools to investigate the role of mitochondria during oxidative stress and neurodegeneration. *Prog. Neurobiol.*, **79**, 136-171 (2006).
63. Ansar, S. ; Abudawood, M. ; Hamed, S.S. and Aleem, M.M. Exposure to Zinc Oxide Nanoparticles Induces Neurotoxicity and Proinflammatory Response: Amelioration by Hesperidin. *Biol. Trace Elem. Res.*, **175**, 360-366 (2017).
64. Kaya, H. and Akbulut, M. Effects of waterborne lead exposure in Mozambique tilapia: Oxidative stress, osmoregulatory responses, and tissue accumulation. *J. Aquat. Anim. Health*, **27**, 77-87 (2015).
65. Wang, C. ; Wu, H.M. ; Jing, X.R. ; Meng, Q. ; Liu, B. ; Zhang, H. and Gao, G.D. Oxidative parameters in the rat brain of chronic mild stress model for depression: relation to anhedonia-like responses. *The Journal of Membrane Biology*, **245**, 675-681 (2012).
66. Baillet, A. ; Chantepedrix, V. ; Trocme, C. ; Casez, P. ; Garrel, C. and Besson, G. The role of oxidative stress in amyotrophic lateral sclerosis and Parkinson's disease. *Neurochemical Research*, **35**, 1530-1537 (2010).
67. Seif, M.M. ; Ahmed-Farid, O.A. and Aboulthana, W.M. Evaluation of the Protective Effect of *Acacia senegal* Extract against di-(2-ethylhexyl phthalate) Induced Hepato- and Neurotoxicity in Rats. *Annual Research & Review in Biology*, **19**, 1-17 (2017).
68. Davies, M.G. ; Fulton, G.J. and Hagen, P.O. Clinical biology of nitric oxide. *Br. J. Surg.*, **82**, 1598-1610 (1995).
69. Ruas, C.B.G. ; Dos Santos Carvalho, C. ; De Araújo, H.S.S. ; Espíndola, E.L.G. and Fernandes, M.N. Oxidative stress biomarkers of exposure in the blood of cichlid species from a metal-contaminated river. *Ecotoxicol. Environ.*, **71**, 86-93 (2008).
70. Afifi, M. ; Saddick, S. and Abu Zinada, O.A. Toxicity of silver nanoparticles on the brain of *Oreochromis niloticus* and *Tilapia zillii*. *Saudi J. Biol. Sci.*, **23**, 754-760 (2016).
71. Senapati, V.A. ; Kumar, A. ; Gupta, G.S. ; Pandey, A.K. and Dhawan, A. ZnO nanoparticles induced inflammatory response and genotoxicity in human blood cells: A mechanistic approach. *Food Chem. Toxicol.*, **85**, 61-70 (2015).
72. Shim, K.H. ; Hulme, J. ; Maeng, E.H. ; Kim, M.K. and An, S.S. Analysis of zinc oxide nanoparticles binding proteins in rat blood and

- brain homogenate. *Int. J. Nanomed.*, **9**, 217-224 (2014).
73. Abdalla, M.S. ; Sharada, H.M. ; Abulyazid, I. ; Abd El Kader, M.A. and Kamel, W.M. Ameliorative effect of salicin against gamma irradiation induced electrophoretic changes in brain tissue in male rats. *UK J. Pharm. Biosci.*, **3**, 29-41 (2015).
74. Sharada, H.M. ; Abdalla, M.S. ; Ibrahim, I.A. ; El Kader, M.A. and Kamel, W.M. Electrophoretic study of the antagonistic effect of salicin isolated from Egyptian willow leaves (*Salix subserrata*) against the effect of gamma irradiation in male rats. *World J. Pharm. Pharm. Sci.*, **4**, 1576-1602 (2015).
75. Aboulthana, W.M. ; Ismael, M. and Farghaly, H.S. Electrophoretic and molecular dynamic evaluation of mutagenicity induced by toxic factors affecting testicular tissue in rats. *International Journal of Current Pharmaceutical Review and Research*, **7**, 319-333 (2016).
76. Hawkins, C.L. ; Morgan, P.E. and Davies, M.J. Quantification of protein modification by oxidants. *Free Radical Biology and Medicine*, **46**, 965-988 (2009).
77. Bass, K.M. ; Newschaffer, C.J. ; Klag, M.J. and Bush, T.L. Plasma lipoprotein levels as predictors of cardiovascular death in women. *Arch. Intern. Med.*, **153**, 2209-2216 (1993).
78. Bonnefont-Rousselot, D. Gamma radiolysis as a tool to study lipoprotein oxidation mechanisms. *Biochimie.*, **86**, 903-911 (2004).
79. Satoh, T. Toxicological implications of esterases-From molecular structures to functions. *Toxicology and Applied Pharmacology*, **207**, 11-18 (2005).
80. Bhatia, A.L. and Manda, K. Study of pre-treatment of melatonin against radiation-induced oxidative stress in mice. *Environ. Toxicol. Pharmacol.*, **18**, 13-20 (2004).
81. De Freitas, R.B. ; Augusti, P.R. ; De Andrade, E.R. ; Rother, F.C. ; Rovani, B.T. ; Quatrin, A. ; Alves, N.M. ; Emanuelli, T. and Bauermann, L.F.J. Black Grape Juice Protects Spleen from Lipid Oxidation Induced by Gamma Radiation in Rats. *Food Biochem.*, **38**, 119-127 (2014).
82. Li, X.L. ; Zhou, A.G. and Li, X.M. Inhibition of *Lycium barbarum* polysaccharides and *Ganoderma lucidum* polysaccharides against oxidative injury induced by γ -irradiation in rat liver mitochondria. *Carbohydrate Polymers*, **69**, 172-178 (2007).
83. Benjamin, S. ; Pradeep, S. ; Josh, M.K.S. ; Kumar, S. and Masai, E. A monograph on the remediation of hazardous phthalates. *J. Hazard Mater.*, **298**, 58-72 (2015).
84. Srividhya, R. ; Gayathri, R. and Kalaiselvi, P. Impact of epigallo catechin-3-gallate on acetylcholine-acetylcholinesterase cycle in aged rat brain. *Neurochemistry International*, **60**, 517-522 (2012).
85. Koitka, M. ; Höchel, J. ; Gieschen, H. and Borchert, H. Improving the ex vivo stability of drug ester compounds in rat and dog serum: Inhibition of the specific esterases and implications on their identity. *Journal of Pharmaceutical and Biomedical Analysis*, **51**, 664-678 (2010).
86. Bedwell, S. ; Dean, R.T. and Jessup, W. The action of defined oxygen centered free radicals on human low-density lipoprotein. *Biochem. J.*, **262**, 707-712 (1989).
87. El-Zayat, E.M. Isoenzyme Pattern and Activity in Oxidative Stress-Induced Hepatocarcinogenesis: The Protective Role of Selenium and Vitamin E. *Research Journal of Medicine and Medical Sciences*, **2**, 62-71 (2007).
88. Milligan, J.R. and Ward, J.F. Yield of single-strand breaks due to attack on DNA by scavenger-derived radicals. *Radiat. Res.*, **137**, 295-299 (1994).
89. Kaneko, T. ; Tahara, S. ; Tanno, M. and Taguchi, T. Effect of age on the induction of 8-oxo-2'-deoxyguanosine-releasing enzyme in rat liver by γ -ray irradiation. *Archives of Gerontology and Geriatrics*, **36**, 23-35 (2003).
90. Ismael, M. and Del Carpio, C.A. Elucidate the origin of CYP flexible structural variation using molecular dynamics calculation. *Journal of Toxicology and Environmental Health Sciences*, **3**, 335-341 (2011).